A Vibrotactile Floor for Enabling Interaction through Walking in Virtual Spaces

Alvin Wing-Hong Law

Department of Electrical & Computer Engineering
McGill University
Montréal, Canada

September 2010

A thesis submitted to McGill University in partial fulfillment of the requirements for the degree of Masters in Engineering.

2010/09/26

Abstract

In existing virtual environments, conventional ground surfaces often impair a user's sense of immersion due to their static nature. This thesis presents a novel approach to enhance one's sense of presence through a floor interface platform that mimics a variety of ground terrains. The ambient system records the force profile of footsteps, synthesizes appropriate responses, and delivers these signals through vibrating floor tiles to imitate the feel and sound of walking on various surfaces. High-quality interactive graphics provided by overhead projectors complete the multimodal experience. Virtual snow and ice environments were developed that allow users to create footprints and crack a frozen ice sheet. Moreover, a perceptual experiment involving the recognition of eight vibration patterns, or haptic icons, delivered to the feet was performed to gauge its discrimination ability. It was found that the interaction afforded to users by the augmented floor was both engaging and perceptually convincing.

Sommaire

A present, dans les milieux virtuels, les surfaces de planchers conventionnelles nuisent à la sensation d'immersion à cause de leur nature statique. Cette thése de recherche propose une approche nouvelle pour améliorer l'expérience de l'utilisateur en utilisant un plancher interactif capable de reproduire plusieurs sortes de terrains. Le système ambiant capte le profile de force appliqué au plancher par les pas de l'utilisateur, synthèse une réponse appropriée et transmet ces signaux à l'aide de tuiles vibrantes ce qui reproduit la sensation tactile et sonore de marcher sur divers types de surfaces. De plus, la surface du plancher est illuminée par des projecteurs suspendus au plafond, permettant la projection de graphiques interactifs et de hautes qualités pour compléter l'expérience multimodale. Par exemple, des environnements virtuels hivernaux permettant aux utilisateurs de laisser leurs traces dans la neige ou de craquer la glace d'un étang gelé ont été développés pour démontrer les capacités du système. De plus, une étude de perception sur la reconnaissance de huit modèles de vibration, ou d'icônes tactiles, transmis par notre plancher pour élucider la capacité de discrimination du pied a permit de découvrir que notre système est perceptivement convaincant et prenant.

Acknowledgments

First of all, I would like to sincerely extend my appreciation to my supervisor, Jeremy R. Cooperstock, for his guidance and discussions over the past two years, and, particularly, for always stressing *the big picture*. This thesis would not have been possible without the work of Yon Visell, who started the project shortly before I joined the Shared Reality and Environments (SRE) Laboratory and continues to guide its development.

I would like to thank Paul Kry and Benjamin Peck, who created the graphics for the snow environment. Much appreciation also goes to Jessica Ip, who helped with the programming for both virtual simulations. Courses taken during my degree with Vincent Hayward, Frank Ferrie, Philipe Depalle, Marcelo Wanderley, and Irene Leszkowicz were all extremely insightful.

The floor platform could not have been constructed within such a short time frame without the help of Michael Mark and Gil Rind. Special thanks to Dalia, Gaurav and all the other SRE lab members for creating an enjoyable work atmosphere.

Finally, I would like to dedicate this thesis to my family - Tammy, Jeannette, Peter and Amy - and to all the friends I have met here in Montréal and back in Vancouver. My sincerest gratitude goes out to all of you.

Funding for this project was provided by the Natural Sciences and Engineering Research Council (NSERC), les Fonds Quebecois de Recherche sur la Nature et les Technologies (FQRNT), and the Canada Foundation for Innovation (CFI).

Contents

1 Introduction **1**
1.1 Virtual Environments . . . 2
1.2 Foot-centered Interaction . . . 3
1.2.1 Locomotion . . . 3
1.3 Literature Review . . . 4
1.3.1 Augmented Floors . . . 4
1.3.2 Augmented Shoes . . . 8
1.4 Overview . . . 8

2 Hardware **11**
2.1 Design Guidelines . . . 11
2.2 First Generation . . . 13
2.3 Actuation . . . 14
2.3.1 Proprioceptive versus tactile sensing . . . 15
2.3.2 Characteristics of vibrotactile motors . . . 15
2.4 Sensing . . . 17
2.4.1 Force Sensors . . . 17
2.4.2 Data Acquisition Units . . . 19
2.4.3 Calibration . . . 20
2.5 Physical Construction . . . 20
2.5.1 Base structure . . . 21
2.5.2 Tile material . . . 25
2.5.3 Suspension . . . 26
2.5.4 Graphical Display . . . 27

2.6 System Architecture 30
2.7 Overall Environment 32

3 Applications **35**
3.1 Haptic-Audio Synthesis 35
3.1.1 Sound Design Tools 36
3.1.2 Available Parameter Adjustments 37
3.2 Snow Simulation 41
3.2.1 Haptic-Audio Rendering of Snow 41
3.2.2 Deformable Terrain Rendering 42
3.2.3 Motion Capture 47
3.2.4 Results 48
3.3 Ice Simulation 48
3.3.1 Haptic-Audio Rendering of Ice 50
3.3.2 Visual Crack Rendering 51
3.3.3 Position Sensing 56
3.3.4 Results 57
3.4 Haptic Icons Underfoot 58
3.4.1 Motivation 59
3.4.2 Background 60
3.4.3 Design of Stimulus Set 61
3.4.4 Methodology 61
3.4.5 Results 62

4 Conclusions and Future Work **67**
4.1 Conclusions 67
4.2 Future Work 70

A User Testing Documents **73**

Bibliography **77**

List of Figures

2.1 Clark Synthesis Tactile Sound Transducer Silver. 16
2.2 A Voltage to Current circuit was used to help linearize the force readings. For stepping forces, we use a value of 150 Ohms for RG. 18
2.3 Top-down view of sensor placement relative to the actuator and the rigid floor tile. 18
2.4 One of the 36 actuated regions. 21
2.5 Base structure provides stability to sensing and actuation components. . . 22
2.6 Dimensions of one row. 23
2.7 Dimensions of the cross-beam pieces. 24
2.8 *Left*: Signal cables from the six sets of FSRs are plugged into the Gluion device. *Right*: Banana plugs provide an easily accessible interface to the actuator units. 24
2.9 Base structure with tiles and border covers. 26
2.10 Three views of the tile with attached rubber supports and tactile sound transducer. 27
2.11 The retainer socket is used to limit the tile's lateral movement. 28
2.12 *Left*: A projected image of small sand hills. *Right*: A projected image of medium sized gravel. 28
2.13 Visuals are provided by dual overhead projectors. 29
2.14 Resulting shadow effect from two overlapping projectors. 30
2.15 A top-down view of the overall placement of components and the logical connections between them. 31
2.16 The rack of haptic-audio synthesis computers and multi-channel audio hardware. 32

2.17 Sketch of the completed construction in the lab's existing VE. It includes three back-projected screens and a set of motion capture cameras. 33
2.18 The completed floor inside the lab's CAVE. 34

3.1 Parameter adjustment GUI for the crumpling model. The values shown are for crushing an aluminum can. 38
3.2 Signal analysis of synthesized feedback with can-crushing parameter settings resulting from one step. *Above*: Vibration waveform. *Below*: Associated spectrogram. 40
3.3 Chosen parameter values for the snow simulation. 43
3.4 Signal analysis of synthesized feedback with snow parameter settings resulting from one step. *Above:* Vibration waveform. *Below:* Associated spectrogram. 44
3.5 The interactive snow field. 45
3.6 *Left*: Simple footsteps. *Middle*: A foot drag. *Right*: A foot swipe. 46
3.7 Vicon markers are attached to the user's feet using an elastic Velcro strap. 47
3.8 A trail of footsteps is left behind by the walker. 49
3.9 Chosen parameter values for the ice simulation. 51
3.10 Signal analysis of synthesized feedback with ice parameter settings resulting from one step. *Above:* Vibration waveform. *Below:* Associated spectrogram. 52
3.11 The interactive frozen pond surface. 53
3.12 *Left*: Nodes of one crack arm and its direction vector. *Right*: Multiple arms of a crack object. 54
3.13 The crack arms propagate outwards from the foot. The lines have been enhanced in the photographs to show the effect. 55
3.14 Branching occurring on the right crack arm. 56
3.15 The cracking pattern is rendered over top of the ice texture. Circles indicate a few instances of fish. 57
3.16 A shatter occurs at one of the crack seed points. 58
3.17 Average correct identification rates across all sessions for each subject. . . 63
3.18 Average correct identification rates across all subjects for each stimulus. . . 64
3.19 Confusion matrix for all subjects indicating number of responses by the darkness of the cell. 64

3.20 Mean recognition rates averaged across all subjects for each session. 65

List of Tables

2.1 Available large vibrotactile transducers. All prices are in USD. 16

3.1 Descriptions of available haptic-audio synthesis parameters. 39

List of Acronyms

ADC	Analog-to-Digital Converter
AWG	American Wire Gauge
BIP	Breaks in Presence
CAVE	Cave Automatic Virtual Environment
EVA	Ethylene Vinyl Acetate
FSR	Force Sensing Resistor
GUI	Graphical User Interface
IR	Infrared
LPC	Linear Predictive Coding
MIDI	Musical Instrument Digital Interface
OSC	Open Sound Control
SDT	Sound Design Tools
STP	Shielded Twisted Pair
UDP	User Datagram Protocol
USB	Universal Serial Bus
VE	Virtual Environment
VR	Virtual Reality

Chapter 1

Introduction

Imagine a scenario in which people are shown a virtual reality (VR) simulation of a beach. They look around and see the sun shining in the sky. They can hear the ocean waves crashing onto the shore and seagulls squawking while circling above. They navigate themselves to the shoreline and walk into the water. Ripples appear as their feet make contact with the water and splashing sounds are heard with their every step.

State of the art VR systems are already capable of delivering a convincing level of realism. However, certain cues remain that disrupt the illusion and remind the users that they are, in fact, in a research centre's lab. These cues are called "breaks in presence" (BIPs) [1]. Users may mention that the ambient temperature did not feel correct or that they felt no breeze. There could be comments that the simulation lacked the ocean's smell or that computers and electronics could be seen. Users may also point out that whether they were walking in sand or water, the ground forces resembled the same standard hard flooring material common to most buildings. They did not sink into the sand nor sense the physical "splash" of stepping into a water puddle.

When placed within a particular scene, users have certain expectations from their sen-

sory system that, when broken, impair their sense of immersion. The main goal of this thesis is to remedy one BIP mentioned above, the static flooring issue, by developing a device that can be controlled to emulate different terrains.

We have prototyped a floor platform that is enhanced with embedded sensing capabilities and feedback in three modalities: haptic, auditory and visual. Although the ground interface is applicable to a variety of fields, we focus on its role in improving existing virtual environments (VE). Our augmented floor can operate as an additional interaction surface or act as a normal rigid platform when not in use.

1.1 Virtual Environments

A VE is a combination of specialized devices and techniques that attempt to transport users completely into a virtual world by recreating the stimuli that they perceive in real-life settings. Detailed 3D graphics recreate objects and surroundings, sounds can emerge from all directions, and sometimes, users can even *feel* what they are looking at.

The improvement of visuals are a major focus of VEs. Through a computer screen, the user is presented with a very limited field of view. This has been addressed in two main ways: using a head-mounted display (HMD) or increasing the screen size.

HMDs are devices with two small embedded screens that are worn over the eyes. The position and orientation of the user's head is tracked and the resulting view for each eye is rendered producing a 3D image. This is an example of pure virtual reality in which everything seen is generated.

In the case of a Cave Automatic Virtual Environment(CAVE) [2], screens several meters wide are arranged in the shape of a cube to completely encompass the user. This is usually achieved by rear-projection to avoid occlusion from the users themselves. The display

that appears on the floor can also be back-projected, but space constraints often require installations to project from above. Advantages and disadvantages to both approaches are described by Buxton and Fitzmaurice [3].

Directional audio can be rendered through either headphones – the usual choice for HMDs – or an array of speakers positioned around the room. Sounds can provide additional cues to support graphics or exist as the focus of interaction [4].

Recreating the reactive forces of virtual objects remains a challenge for a variety of reasons. Unlike visual and auditory feedback, the sense of touch cannot be perceived at a distance. The user must make a conscious effort to be in contact with a physical device in order to receive feedback in this modality.

1.2 Foot-centered Interaction

Since haptic devices must be touching the body part it wishes to affect, it is difficult to guarantee that the user will perceive the feedback at all assuming the contact is voluntary. Moreover, few regions of the body are accustomed to being used for interaction purposes. The hands are one such body part and the majority of haptics research revolves around taking advantage of their sensitivity. However, one could argue that the feet are in regular contact with the environment more often than the hands. It is surprising that foot-centered haptics constitutes a small percentage of investigation in this field.

1.2.1 Locomotion

Walking is an integral part of familiarizing oneself with a new environment. In addition to providing new vantage points such as navigating around a corner, information is gathered through the act of walking itself. For example, in a field of large stones, it may be difficult

to assess its stability purely through vision. A few steps could inform the walker whether it would be wise to retreat. The firmness of stepping on a snow-covered ground could provide information about the temperature of when the snow fell or if it had been previously compacted. People have acquired a lifetime's worth of experience in discriminating different textures through foot contact.

1.3 Literature Review

The idea of augmented foot-based interaction is not entirely new. This section describes previous related projects and explains why their implementations, which inspire components of our design, do not completely satisfy our objectives. There have been two main approaches to such previous research efforts: augmented floors and augmented shoes.

1.3.1 Augmented Floors

Early publications of sensor-augmented floors emerged from music technology and performance research [5]. Their goals were to create unique instruments and controllers that could facilitate gestural interactions with audio feedback. It is important to note that all of the following floor-based interfaces supported and encouraged multiple simultaneous users.

Pinkston *et al.* [6] created a touch-sensitive dance floor that provided auditory feedback. It functioned similarly to a large keyboard on the ground where performers could affect the music by stepping onto designated regions. They used large force sensing resistor (FSR) sheets to detect foot pressure and relayed the data through Musical Instrument Digital Interface (MIDI) messages.

The Magic Carpet by Paradiso *et al.* [7] extended the musical controller concept to full body motion. Doppler radars sensed upper body movements and a grid of piezoelectric

wires embedded underneath a carpet was used to sense foot pressure and position. Movements by performers were translated into expressive sound. Feedback was purely auditory and delivered through speakers mounted on stands.

While demonstrating an interesting form of user input, a musical instrument metaphor makes it somewhat difficult to evaluate success, partly due to its artistic nature. In contrast, our application domain of terrain simulation focused on feedback that users have already experienced in their lives. Inline with this theme, the PhOLIEMat project developed by Cook [8] used a force sensitive mat to drive a physically based synthesis engine to produce walking sounds. The project's goal was to create a tool that would allow Foley artists to score video that involved walking in noisy terrains quickly, but accurately. The particle-based statistical algorithm relied on the analysis of pre-recorded footsteps in the target material.

The next few projects focused mainly on exploring the variety of sensing techniques available for capturing foot pressures.

Griffith *et al.* [9] created Litefoot using optical proximity sensing. Their project recorded rapid dance movements and achieved a resolution of 4 cm $\times$ 4 cm per sensor at a sampling rate of 100 Hz over an area of 1.76 m^2. However, their optical sensors recorded data in binary and weight distributions were not captured.

Orr and Abowd [10] created the Smart Floor for identifying people based on matching footstep force profiles. They claimed a recognition rate of 93% between 15 subjects even through varying footwear. To capture precise ground reaction forces, they placed four load cells at the corners of a steel plate. The data was then transformed into a ten-dimensional feature space and matched to previously gathered training data. There was no indication of interactive feedback.

Using multiple tiles of the same sensing setup as the Smart Floor, Headon and Curwen

[11] explored the recognition of human movements for ubiquitous gaming. Their sample applications included a game in which a player moves to a specific tile after seeing a visual location cue on a screen. Another application was navigating a first-person shooter by mapping specific tiles to directional keys.

A project known as Z-tiles [12] was developed to allow for interactive floor spaces of reconfigurable shapes and sizes. Each Z-tile consisted of twenty hexagonal force sensing resistors with a resolution of 4 cm $\times$ 4 cm per sensor at 100 Hz. The shape of the Z-tile was unique in that it allowed the tiles to interlock with one another. Through spring-loaded connections, the micro-controllers in each tile communicated with their adjacent neighbours. Setup did not require stringing connection wires and each tile was interchangeable with the next. Their example applications were floor-based music control and movement through VEs by leaning.

A significant increase in resolution and sampling rate was achieved by Srinivasan *et al.* [13]. Their project captured extremely accurate pressure and position information of human locomotion. The floor was assembled out of individual mats, which could operate collectively with a host computer through network switches. Each mat (62 cm $\times$ 53 cm) contained 2016 FSRs that resulted in a resolution of 6 mm $\times$ 6 mm per sensor. Force readings were captured by an Ethernet-enabled micro-controller at 30 Hz. The floor mats were part of a system that included auditory sensing and motion capture. Simple visualization of the force values was available as feedback.

Up to this point, the projects were developed using a controller metaphor. Gestures performed on the floor would trigger events in another location. Instead, we were looking for systems that took advantage of co-located input and response, much like table-top interfaces such as the Reactable [14].

A large-scale luminous floor, named Ada [15], which offered embedded sensing and

output, was publicly exhibited. A total of 360 translucent tiles covered an area of 136 m^2. Each tile consisted of three FSRs and dimmable red, green and blue lights. Their software tracked multiple simultaneous users and created dynamic, though low resolution, visual effects around them.

The iFloor [16] introduced a collaborative floor space by mounting a downward-facing projector and webcam on the ceiling. The floor facilitated a debate through SMS phone messages between users who were confined to the borders of the display. This was done so that shadows from their bodies would not occlude the visuals.

Similar systems to the iFloor have been used for advertisement purposes and exhibited at various malls although we are not aware of any directly related publications. [1] Examples of applications included leaves blowing away from underneath where people walk and kicking a virtual soccer ball by pointing feet over the ball graphic. Shadows were persistent but did not interfere with the goal of attracting attention from the general public.

The Wisdom Well [17] avoided the shadow problem through back-projection. The system consisted of a 3 m $\times$ 4 m $\times$ 3 m sub-floor chamber that housed four projectors and four webcams pointed upwards. The flooring was constructed out of 9 mm glass and a 3 mm Fresnel diffusion layer. The diffusion layer created a surface for the projectors to focus onto yet allowed ambient light from above to pass through. Limbs of users in contact with the floor occluded the light and were captured as dark spots by the webcam. Auditory feedback was provided through ceiling-mounted speakers. The applications focused on multi-player and co-located collaborative games. One scenario required players to traverse a water surface by stepping only on designated *safe* virtual stones. There was no mention of haptic feedback or force sensing.

1. www.displax.com, www.vertigo-systems.com, www.intouchmediagrp.ca

1.3.2 Augmented Shoes

Shoe-based sensing and actuation offer another approach to mediate interaction through walking. They are portable and the user is not constrained by the size of the active sensing area. The first such device was the CyberShoe [18]. Three FSRs were placed in the toe area of the shoe and one was placed in the heel. A state-transition model of toe and heel pressures was used to recognize walking gestures that translated the rendered VR setting around the user.

Paradiso *et al.* [19] created a sneaker instrumented with a variety of sensors that broadcast signals via radio frequency to a base-station. On-shoe sensors included three piezoelectric pressure sensors, a resistive bend sensor, two multi-axis accelerometers, an electromechanical compass, a gyroscope, a sonar transducer, and an electric-field-sensing electrode. Altogether, the shoe measured 14 different parameters and was used for sonic control through dance movements.

Vibrotactile actuators embedded inside shoes have been explored by several projects [20] [21] [22]. The type of vibrations sensed would correspond to a pre-defined meaning. Although promising as a means of delivering arbitrary stimuli to the foot, we felt that the small actuators in shoes limited the range of forces that would be required to mimic the sensations our feet experience on a daily basis.

1.4 Overview

Overall, many types of sensing have been developed and shown to work robustly. System response in the form of simple graphics, musical sounds and in-shoe vibrations have also been explored. However, none of the projects thus far have combined detailed force and location sensing with high-quality feedback in all three modalities. Our implementation of

an intelligent foot-centered device aims to address this shortcoming.

The remainder of this thesis is organized as follows. Details of the design principles and physical construction of the floor, including sensing and actuation considerations, are presented in Chapter 2. In Chapter 3, descriptions of two interactive VE implementations, snow and ice, are presented. Also, Chapter 3 describes a pattern recognition experiment in which eight unique vibrations are delivered to the participant's feet through our floor device. Finally, conclusions and possible future work are presented in Chapter 4.

Chapter 2

Hardware

2.1 Design Guidelines

This chapter will present the specifications of the augmented floor's final design and construction. The choice to pursue a floor-based approach, as opposed to augmented shoes, was made for the following reasons. Floor interfaces have been prototyped many times already and shown to be reliable. Augmented floors offer a more ambient type of interaction because they form part of the environment. We also had concerns about the durability of wearable computing equipment when used by an untrained audience.

The following is a set of design goals that guided that development of this project and addressed some elements absent from previous work done in this domain.

- **Display haptic feedback.** As discussed in Section 1.3.1, all previous floor installations for VEs have neglected the role of active haptic feedback. We consider support for such feedback as the top priority guiding the remainder of the design decisions.
- **Display auditory feedback.** The floor interface should display auditory feedback as well. Almost all VR systems already include this in the form of speakers or head-

phones. Although conventional approaches are sufficient to convey certain sounds such as background noises and generic feedback beeps, localization remains challenging. An engaging simulation would not recreate the sounds of walking through a speaker that is mounted on a stand; rather, the feedback should come from directly underneath the area of the foot. An informal observation from Visell *et al.* [23] indicated that a separation distance of 30 cm between haptic and auditory signals was enough to disrupt the illusion of co-located feedback.

- **Display visual feedback.** Immersion would not be complete without somehow incorporating graphics to supplement the haptic and auditory feedback. In keeping with the theme of localized feedback, the interactive visuals must be displayed directly on the ground, instead of on a screen in front of the user. Graphics are necessary to convey the current state of the entire interaction surface, since haptic and auditory feedback are mainly confined to the immediate area surrounding the users' feet.
- **Have sensing capabilities.** Any interactive system must be able to sense changes in the environment caused by the user. That change can range from a simple button click to a complicated series of steps. Ideally, the sensors should be contained within the floor itself, such that they capture natural footstep force profiles without users tuning their walking habits to the visible sensor devices.
- **Low-latency control loop between sensing and feedback.** High-latency between sensing a change from the user and delivering feedback would result in a low quality experience. As this interaction includes active haptics, latencies in the order of milliseconds are desirable [24]. Visual and auditory feedback need to feel instantaneous and be perceived simultaneously with the haptics.
- **Scale to large areas.** When dealing with locomotion, larger areas are usually preferred. It would be uninteresting for a user to reach the physical boundary of

the device in one step. There has been research into omnidirectional treadmills, but none have perfected the illusion of exploring an indefinitely large area. We decided to pursue expandability through the use of readily available materials, to keep costs low without sacrificing quality.

- **Be stable and durable.** Due to the nature of the interaction (people walking on the device), the design must be stable. A shaky platform would quickly become the focus of the user when the interaction should be taking precedence. We want our device to be enjoyable to use. Durability is also critical because the system must withstand the potential forces of human bodies jumping up and down repeatedly.
- **Accommodate multiple people simultaneously.** Although designing for one user is easier, many possibilities exist for the floor to act as a mediator between multiple users. Sensor and feedback designs should be localized to multiple regions that can operate independently and concurrently.
- **No additional equipment worn by the user.** We want our device to be interactive without requiring the user to wear or hold any additional equipment. Walking on the device should be as natural and unconstrained as possible.

2.2 First Generation

Visell *et al.* [23] prototyped a small floor component named the EcoTile. Their goal was to explore the possibilities of using a linear actuator connected to a rigid surface in order to simulate walking on various materials. When a user stepped onto the tile, the actuator excited the surface such that the forces delivered back to the user's foot were similar to the forces delivered by stepping onto the real material.

A D-Box motion control actuator[1] was used to physically displace two 34 cm × 34 cm plywood tiles in the vertical direction. Sandwiched in between the two tiles were four force sensing resistors (FSRs) encased in foam and connected to a micro-controller (Wiring board) that relayed the force readings through a Universal Serial Bus (USB) connection to a computer. The computer used the force readings to generate haptic signals that were sent to the motion controller and audio signals that were sent to a speaker placed next to the D-Box unit.

The informal results from this first prototype indicated that the feedback delivered was sufficient to give the impression of a drastically different material, e.g., snow, from the one onto which the user actually stepped, a piece of plywood. The success of this prototype motivated the continuation and expansion of the project. Improvements were made in almost all areas of the design; these will be described in detail throughout the remainder of this chapter.

2.3 Actuation

Although haptic and auditory feedback were realized in the first prototype, there were disadvantages to this approach. The control interface induced a latency of over 100 ms. This delay time would inhibit certain terrains, especially hard surfaces, from being simulated properly. These linear motor units required considerable physical space and were quite expensive, limiting opportunities for expansion. The decision was made to move to a vibrotactile actuator that, despite sacrificing the ability to displace the tile vertically, offered many advantages in resolution, latency and cost.

1. www.d-box.com

2.3.1 Proprioceptive versus tactile sensing

Proprioception is a person's sense of their current physical position. This sense informs a person of joint angles or of whole body accelerations, such as sinking into sand. In contrast, tactile sensing allows for the awareness of vibrations on the skin. Both sensations are important in the field of haptics; however, they are each simulated differently. An example of a device providing proprioceptive feedback is the Sensable Phantom.[2] The D-Box actuator also falls into this category, delivering the low frequency, including steady-state, types of feedback such as physical displacement, whereas tactile feedback operates at higher frequencies. A common example of tactile feedback is the eccentric motor contained in most cellphones. Vibrotactile devices are low cost and simple to operate.

A well-designed proprioceptive feedback device with a wide bandwidth of operation would be superior to its vibrotactile counterpart; however, proprioception may not always be necessary. Studies have shown that, for certain tasks such as material identification or impact haptics, information encoded into the higher frequency transients factors more into the users' perception [25] [26].

2.3.2 Characteristics of vibrotactile motors

The two main types of tactile transducers are eccentric motors and vibrotactile inertial motors. The main difference between the two is that eccentric motors do not have independent control over frequency and amplitude. Inertial voice coil motors operate in a similar manner to loudspeakers and thus support a much wider range of haptic signals. The type of vibration felt when placing one's hand against a pulsing sub-woofer diaphragm is a rough approximation to how these devices deliver haptic feedback. Their simple driving

2. www.sensable.com

mechanism means that they are robust, low-cost, low-latency, and easily interfaced with other components.

Table 2.1 Available large vibrotactile transducers. All prices are in USD.

Name	Size(H×W in cm)	Freq. Range	Power (Max.)	MSRP
Aura Pro Bass Shaker	5×15	20-100 Hz	75 W	$120
Buttkicker BK-LFE	13.5×14	5-200 Hz	1500 W	$230
SIT IBEAM VT300	7×16.5	20-800 Hz	250 W	$350
Buttkicker BK-Mini-LFE	7.62×12	5-200 Hz	250 W	$80
Clark Synthesis Silver	6×20.5	15 Hz-17 kHz	350 W	$150
Clark Synthesis Gold	6×20.5	10 Hz-17 kHz	400 W	$350
Clark Synthesis Platinum	6×20.5	5 Hz-17 kHz	400 W	$450

Figure 2.1 Clark Synthesis Tactile Sound Transducer Silver.

The tactile transducer chosen for this project was the Clark Synthesis TST239 Silver, seen in Figure 2.1. It originally was designed as an enhancement to home-theatre systems for users to attach to the undersides of their couches. Its frequency response is rated from 15 Hz to 17 kHz and requires an audio amplifier capable of delivering at least 75 W at 4 ohms. The frequency range is especially important as it includes most of the human audible range (20 Hz to 20 kHz). This means that in addition to displaying the haptic feedback, the same device can be used simultaneously for auditory feedback. To transmit the vibrations

to the user's feet, the actuator would need to be attached under a rigid platform that could support a person standing on top.

2.4 Sensing

In many VEs, whole-body tracking can be achieved using motion capture systems that match on-body markers with a predefined human model. However, these systems are unable to capture detailed foot-ground forces, which will constitute the majority of the interactions in this project. In a given body pose, a user can adjust the foot, and even the part of the foot, that will be the weight bearing area without shifting the rest of the body. Thus, we explore sensing options that provide a real-time force map of the interaction area. Although we would like to sense as many foot-ground force orientations as possible, we began by tracking forces applied directly downwards.

2.4.1 Force Sensors

Similar to the augmented floors described in Section 1.3.1, our options for force sensors are between load cells and force-sensing resistors. Load cells can provide precise and repeatable measurements. However, they can cost about ten times as much as FSRs, which hinder considerations for sensing resolution and expandability. Since we do not need exact force measurements for recognizing specific walker profiles, we opt for FSRs. The increased resolution that can be gained affordably by the addition of more sensors in a given area outweigh technical accuracy.

The floor is outfitted with Interlink model 402 FSRs. Due to the large variation in characteristics between each sensor (manufacturer quoted 25% variance in readings), each FSR needs to be calibrated individually. The circuit seen in Figure 2.2 also helps to linearize

the force response.

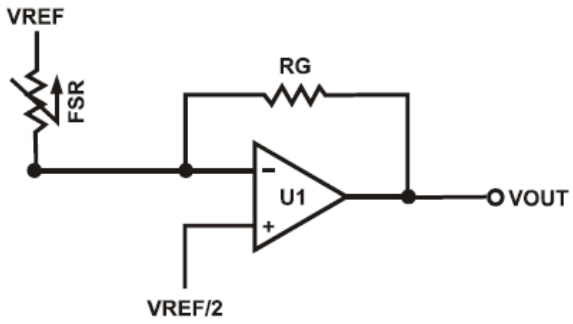

Figure 2.2 A Voltage to Current circuit was used to help linearize the force readings. For stepping forces, we use a value of 150 Ohms for RG.

Placement

To sense ground reaction forces, the force sensors need to be underneath the rigid flooring. We choose to place the sensors at the four corners of each tile as seen in Figure 2.3.

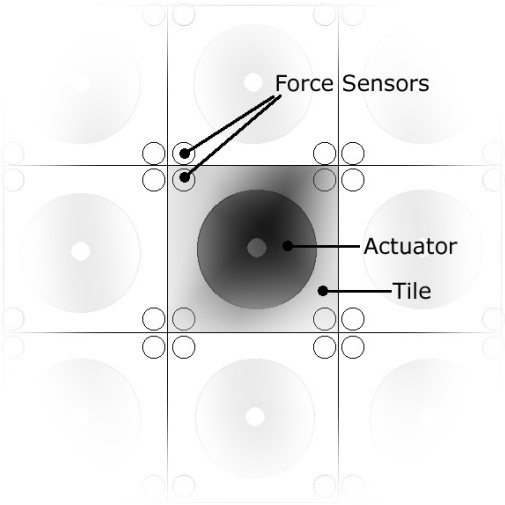

Figure 2.3 Top-down view of sensor placement relative to the actuator and the rigid floor tile.

This configuration allows for interpolation of the center of pressure on each tile and also provides the greatest physical stability. Moving the sensors inwards causes undesirable lifting of the tile when weight is applied to the edges.

2.4.2 Data Acquisition Units

The analog sensor signals from the FSRs are digitized and sent to the computer. A micro-controller samples FSR voltages and converts them to integer values. The resolution of conversion depends on the bit-rate of the micro-controller's analog-to-digital converter (ADC).

Arduino and Wiring boards

The initial prototype floors capture force data using these basic micro-controller devices. Arduino Diecimila and Wiring boards [3] both have 10-bit ADCs and communicate input/output signals with the host through serial protocol over USB. Analog inputs are limited to eight for the Wiring board and six for the Arduino; adding multiplexers to increase the number of inputs would slow down the sampling rate considerably.

Gluion units

A major upgrade to the previous data acquisition units is a custom-built 32-channel board based on the Altera FPGA. These Gluion [4] units contain 16-bit ADCs, sampling at a rate of 1 kHz. The board also incorporates a 10 Mbps Ethernet interface and broadcasts data via User Datagram Protocol (UDP) using the Open Sound Control (OSC) protocol. [5]

3. www.arduino.cc, www.wiring.org.co
4. www.glui.de
5. www.opensoundcontrol.org

Ethernet connectivity provides a clean and simple mechanism to connect an array of Gluions to an array of computers.

The force sensors are connected to the Gluions through XLR connectors. This makes for easy and secure re-connections during setup and troubleshooting. Each XLR plug contains five channels: one ground and four signals, enough for a single tile. Custom-length cables are built using shielded twisted pair (STP) cable containing four pairs of 24 American Wire Gauge (AWG) insulated wiring. At one end, each twisted pair of wires is connected to the leads of the FSR. At the other end, all the white wires are soldered onto the ground lead while the colored wires are connected to the signal leads.

2.4.3 Calibration

Each FSR should be individually calibrated. This can be performed using a small set of known weights and linear regression fitting. For more precise calibration, many more sample points can be taken using a load-cell in series with the FSR while the force applied is constantly increased. Using this method, a response accurate to within 5% can be achieved.

2.5 Physical Construction

Our design is largely constrained by the 20.3 cm diameter of the actuator. For convenience, we choose a standard tile size of 30 cm $\times$ 30 cm to match the existing tiles in the building. At this dimension, a user's two feet are unlikely to be on the same tile during locomotion. If one foot overlaps on a the tile already in use by the other foot, both feet will perceive the same vibrations. However, the active stepping foot would experience stronger vibrations due to the pressure distribution between the feet during a step. This could be perceived as increased actuation resolution.

The CAVE dimensions, in which the hardware is deployed, allow for a maximum floor area of 2.4 m × 2.4 m. Users often confine themselves to the center of this space and rarely approach the sides, which helps to minimize the risk of slipping and damage to the screens. We therefore restrict the *effective* interaction area of the floor to the inner 1.8 m × 1.8 m square with 36 independent regions. Figure 2.4 illustrates a one-tile abstraction, which includes the rubber suspension that will be explained in Section 2.5.3.

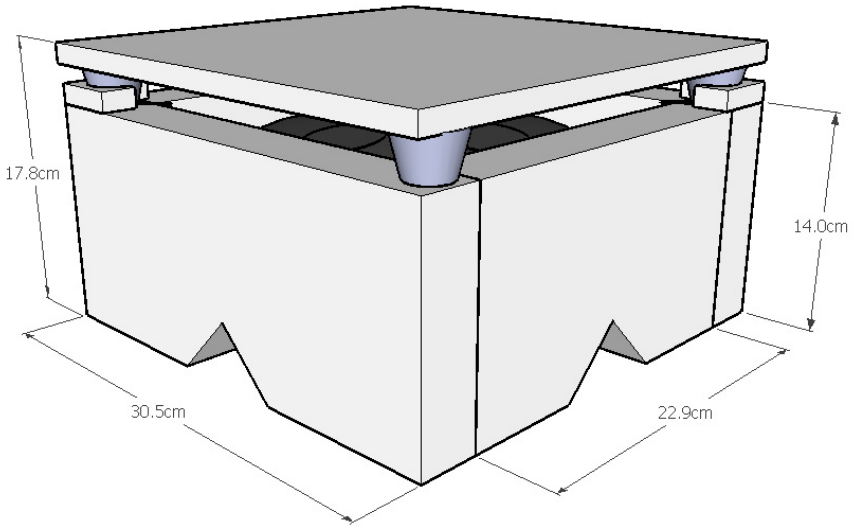

Figure 2.4 One of the 36 actuated regions.

2.5.1 Base structure

A stable support structure is required to hold the actuators and sensors in place. It serves as a simple raised flooring support similar to those found in computer server rooms. The base, seen in Figure 2.5, is built with affordable housing construction wooden beams. Triangular notches are cut into the beams to allow wiring to run between the chambers and the structure is secured to the lab floor for extra stability.

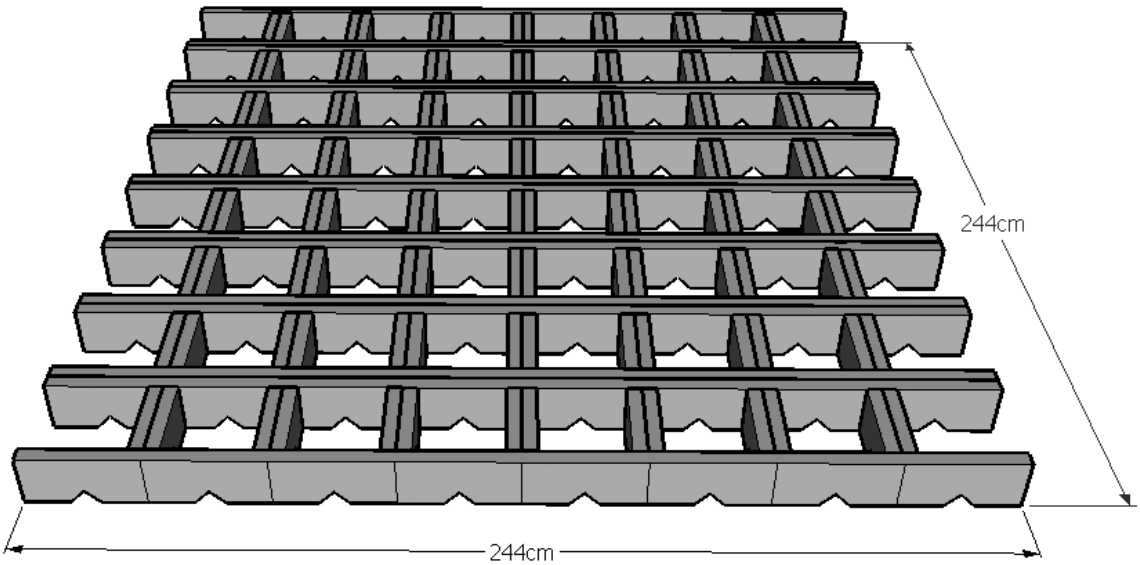

Figure 2.5 Base structure provides stability to sensing and actuation components.

The structure consists of eight individual rows that are bolted together. Each row contains eight chambers of volume 23 cm × 23 cm × 14 cm to accommodate the transducers and is constructed with two beams 2.4 m long and a series of small cross-beam pieces. Detailed dimensions are seen in Figure 2.6 and Figure 2.7.

The two end chambers of each row are used to house sensitive electronics and connections. This provides some protection from repeated usage and helps to abstract the underlying technology from the user. Keeping the end chambers open also allows easy access to the embedded sensors and actuator wiring without having to open the tiles from the middle of the floor, which would then require recalibration of the sensors. Actuator leads are terminated at one end through standard audio banana plugs and FSR cables are connected at the other end into the Gluion box as seen in Figure 2.8.

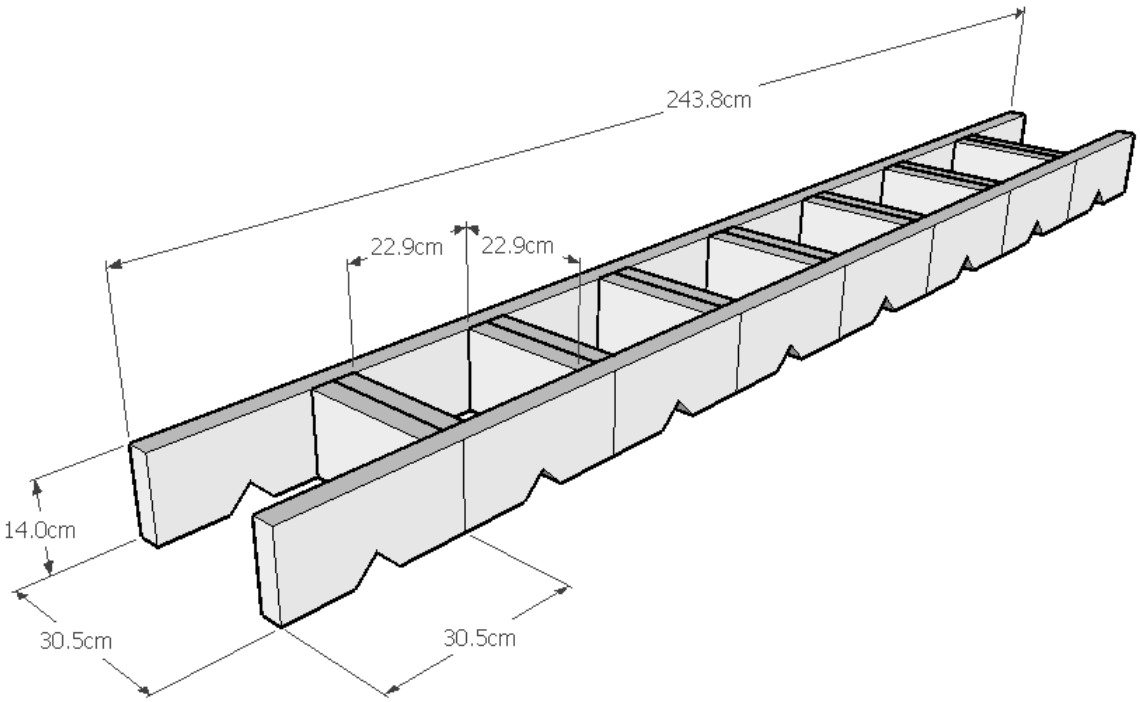

Figure 2.6 Dimensions of one row.

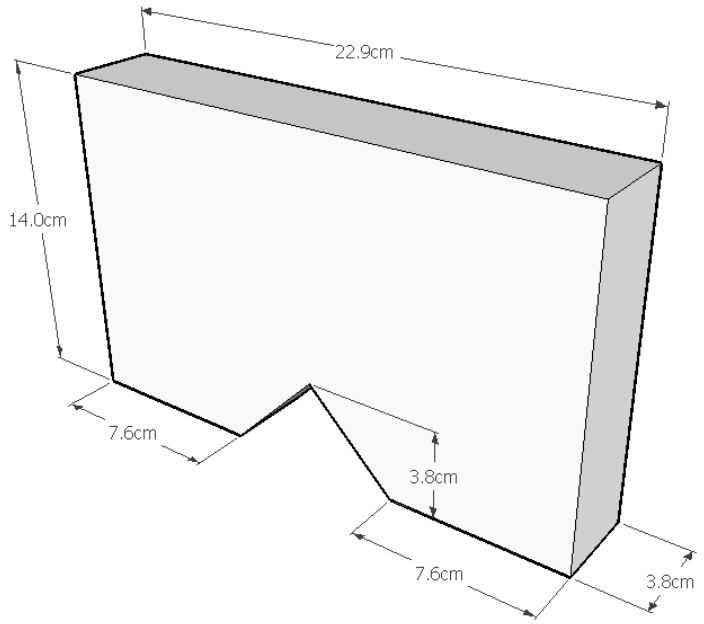

Figure 2.7 Dimensions of the cross-beam pieces.

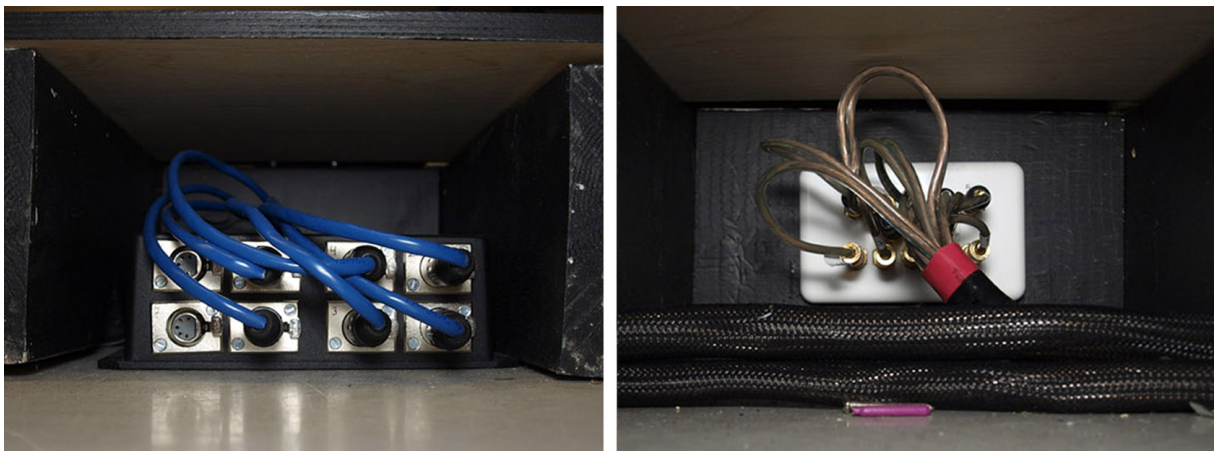

Figure 2.8 *Left*: Signal cables from the six sets of FSRs are plugged into the Gluion device. *Right*: Banana plugs provide an easily accessible interface to the actuator units.

2.5.2 Tile material

The top layer of the floor is constructed with a stiff material. The actuators are connected to the tile with a supplied aluminum plate. For the vibrations to be transmitted most efficiently to the foot, the connection must be as rigid as possible. On the 2 × 2 prototype, 1.25 cm thick transparent polycarbonate was used mainly for aesthetic reasons. Users could see through the tiles to the components hidden beneath. Perceptually, however, the differences between delivering the haptic and auditory feedback through polycarbonate versus plywood are difficult to notice and can be compensated by the signal synthesis. Moreover, the aesthetic appeal of the transparent tiles was lost when an opaque covering was used to support graphical projection.

Our floor uses 36 Russian Birch plywood tiles of dimension 30 cm × 30 cm × 1.25 cm. This leaves a gap of 3 mm between adjacent tiles to help isolate vibrations. Strips of foam are taped to the sides of the tiles to fill these gaps and create a seamless screen on which to project graphics. The tiles were covered with a specially formulated paint for high reflectivity.[6] We used Goo Systems' Digital Grey for the undercoat and their Rear Projection paint for the topcoat. Though the latter was reputed for durability, we found that it was easily scuffed by regular usage. Two layers of matte varnish were added on top, which reduced the reflectivity of the surface, but made the floor less susceptible to marking. The grey colour of the paint is intended to enhance the contrast of the resulting picture in situations where ambient light is present. A white floor would only perform well in a much darker room.

The outer border surrounding the active tiles is fitted with long planks of the same plywood used for the tiles. The planks are secured in place by Velcro strips and can be

6. www.goosystems.com

easily removed to access the connection ports. Black paint covers both the base structure and the side planks to distinguish the inactive from the active areas, as seen in Figure 2.9.

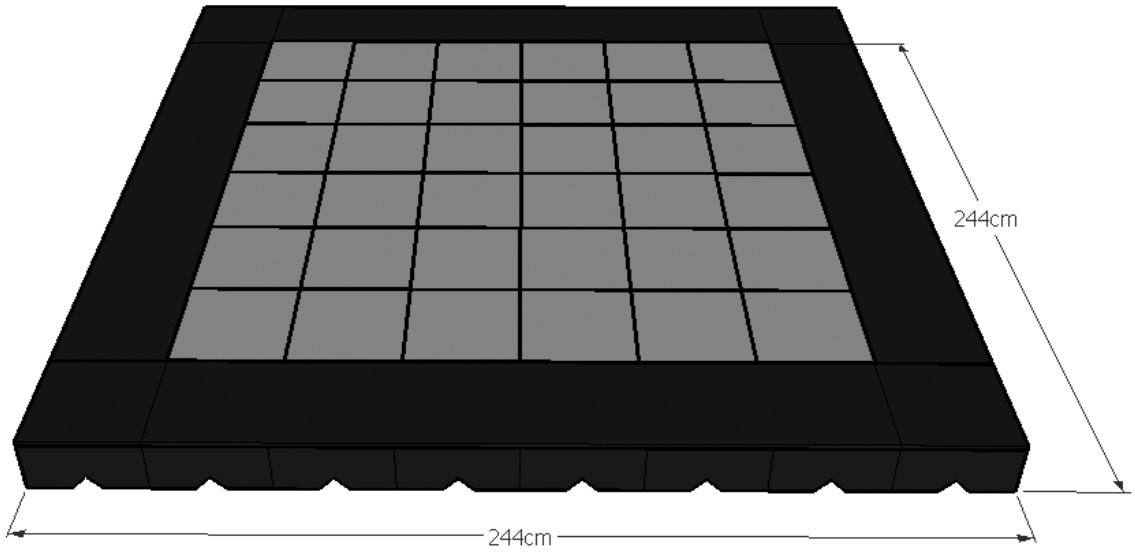

Figure 2.9 Base structure with tiles and border covers.

2.5.3 Suspension

To ensure a smooth response from the force sensors, the manufacturer recommends encasing them between a soft material such as rubber or foam. The majority of implementations we came across used a closed cell ethylene vinyl acetate (EVA) foam. Applying this suspension technique in the first generation prototype under the load of a human weight, we found that there was too much compliance when the foam was only located at the sensor points. In the second generation prototype, we use a ring of foam around the edge of the tile. The ring also acts as a retainer to keep the tile from shifting horizontally and skewing the force readings. This is accomplished by gluing alternating sections of foam to the tile and to the supports. Although it is more rigid, this design spreads the forces from the tile

around the ring and we lose precision in interpolating force contact positions.

Reverting to the original design of only supporting the tile at the corners, we replaced the EVA foam with a stiffer material. Each tile is supported by four cylindrical SBR rubber stoppers, attached to the tile's underside with 3M silicon glue as seen in Figure 2.10. Each FSR is lightly glued into place on top of a thin rubber sheet that is attached to the platform. The sensor rests between the rubber sheet below, and rubber stopper above. In order to prevent the tile from shifting, wooden retainer sockets are manufactured and nailed to the platform surrounding the FSR, as seen in Figure 2.11. Two sockets placed at opposing corners sufficiently constrain each tile.

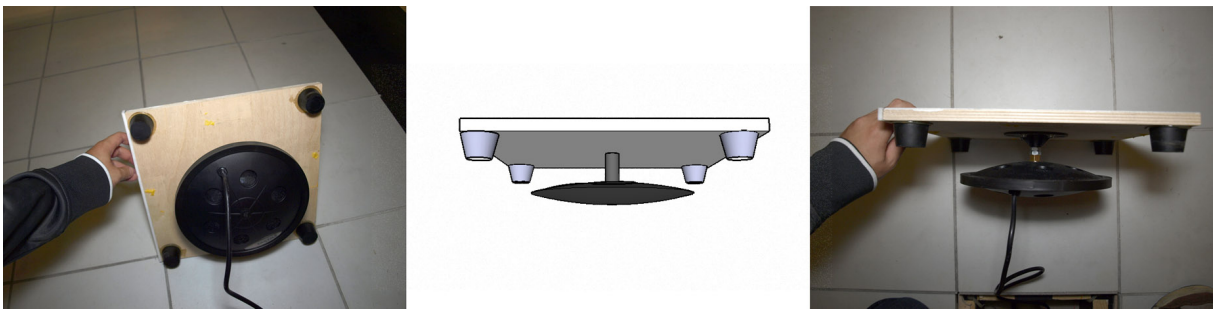

Figure 2.10 Three views of the tile with attached rubber supports and tactile sound transducer.

2.5.4 Graphical Display

Rendering graphical feedback directly on the floor was a challenge. The maximum visual acuity achievable by the human eye is about 50 cycles per degree [27], equivalent to the ability to distinguish black and white bars, an extreme case of contrasting stimuli, that subtend an angle of 1.2 arc-minutes. At a standing height of 170 cm, a person with perfect vision under ideal conditions can resolve features as small as 0.6 mm. For many natural ground surfaces, visual characteristics tend to vary gradually and thus, even the modest resolution of an affordable XGA projector may be sufficient. At a projected area

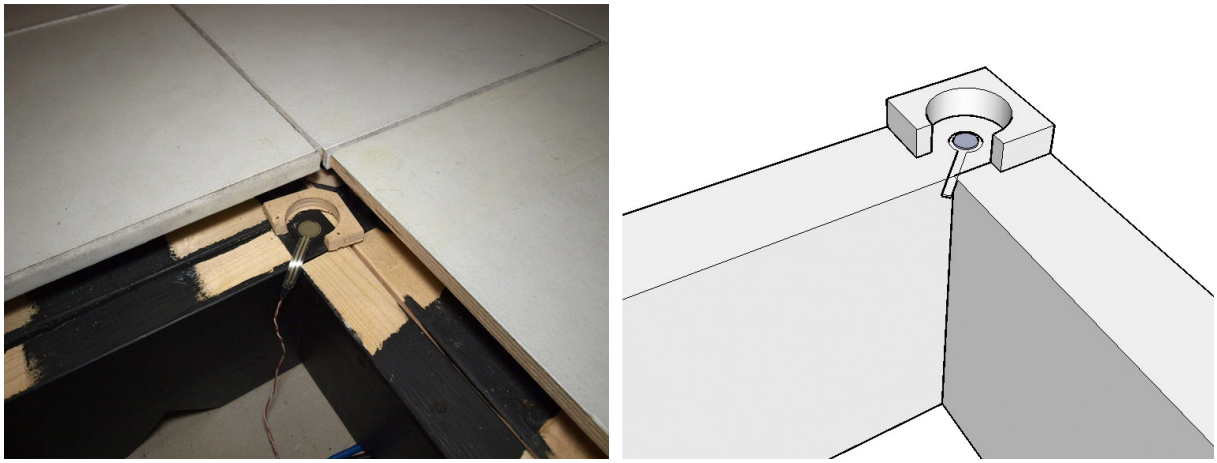

Figure 2.11 The retainer socket is used to limit the tile's lateral movement.

of 1.8 m × 1.8 m, 768 pixels per dimension correspond to a pixel size of 2.3 mm. Though well short of the 0.6 mm limit, the apparent ground texture resolution was nevertheless perfectly adequate to display complex terrains, as seen in Figure 2.12.

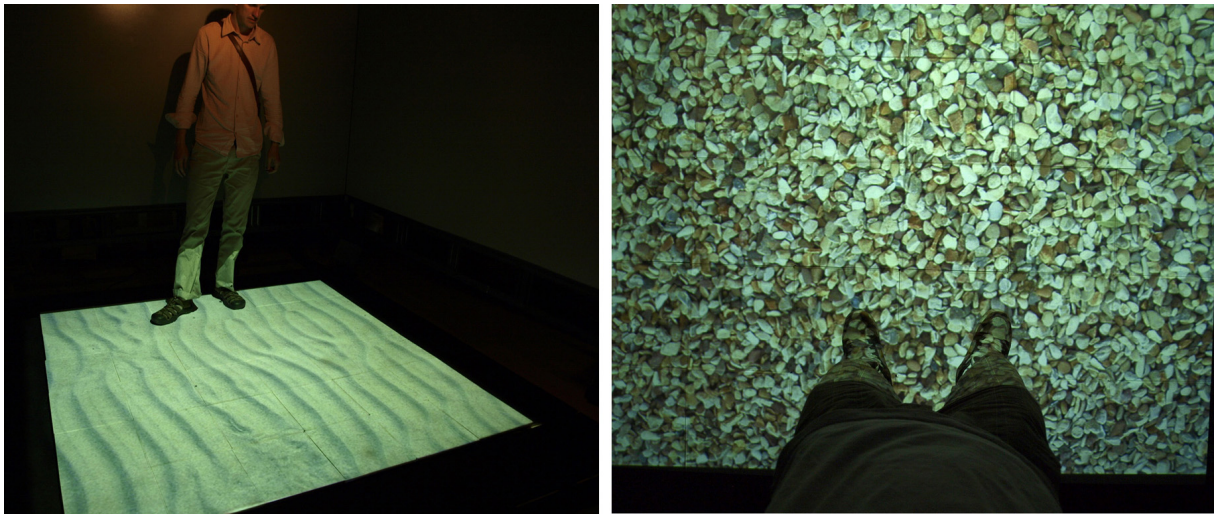

Figure 2.12 *Left*: A projected image of small sand hills. *Right*: A projected image of medium sized gravel.

Although we would have preferred to use the shadowless back projection implementation of the StepStone project [17], this was not feasible because the force sensors and actuation

units would have occluded most of the light. We resorted to using top-down projection, which made our setup more adaptable to existing infrastructure as the floor would not require a large clearance underneath. However, we must consider the need to preserve visibility of graphical deformation in the vicinity of the user, which may be occluded by shadow. Our solution was to employ two overlapping projectors (Hitachi CPX-5), seen in Figure 2.13. Although this form of passive shadow reduction does not entirely eliminate the problem, shadows appear as dimmer regions of the terrain rather than as entirely occluded regions. To a certain extent, this setup is perceptually acceptable as it preserves some of the characteristics of natural illumination. Figure 2.14 shows the resulting effect of occlusion from a user's point of view.

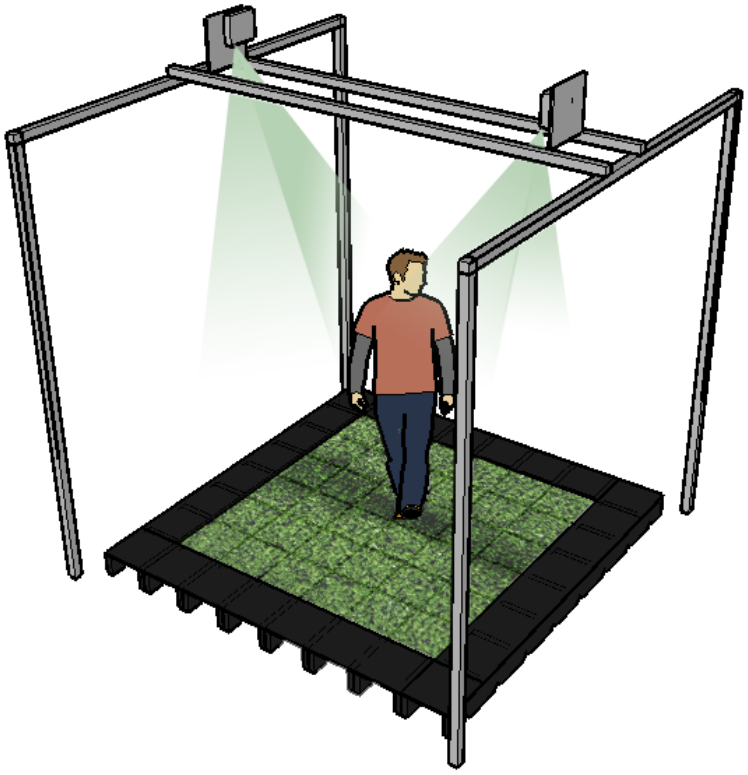

Figure 2.13 Visuals are provided by dual overhead projectors.

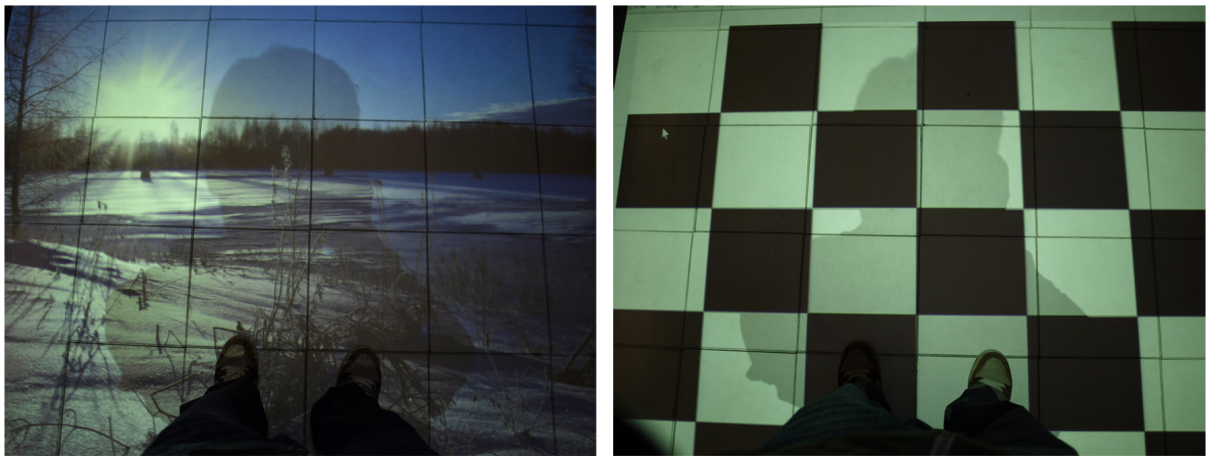

Figure 2.14 Resulting shadow effect from two overlapping projectors.

2.6 System Architecture

An overview of the signal connections between the various components can be seen in Figure 2.15. The system transfers data on a Gigabit Ethernet network, via two 8-port switches. Connected to the first switch are six Gluion sensor boxes, the FPGA-based devices responsible for capturing force readings from the tiles. The sound synthesis software, described in Section 3.1, runs on an array of six Mac Mini computers networked together on the second switch. Each PC is responsible for generating feedback for one row of six tiles. We limited the maximum number of associated tiles with each PC in the case that we implement new, more computationally costly physical models. The drawback of this architecture is the added complexity of creating a central control interface. Additional sub-systems of the complete VR environment setup are the motion capture system and the real-time graphics system. These components will be described in Section 3.2.

Each PC delivers six audio signals through an Edirol FA-101 Firewire external sound card. The signals are then amplified by a Russound 1250MC 12-channel amplifier, which

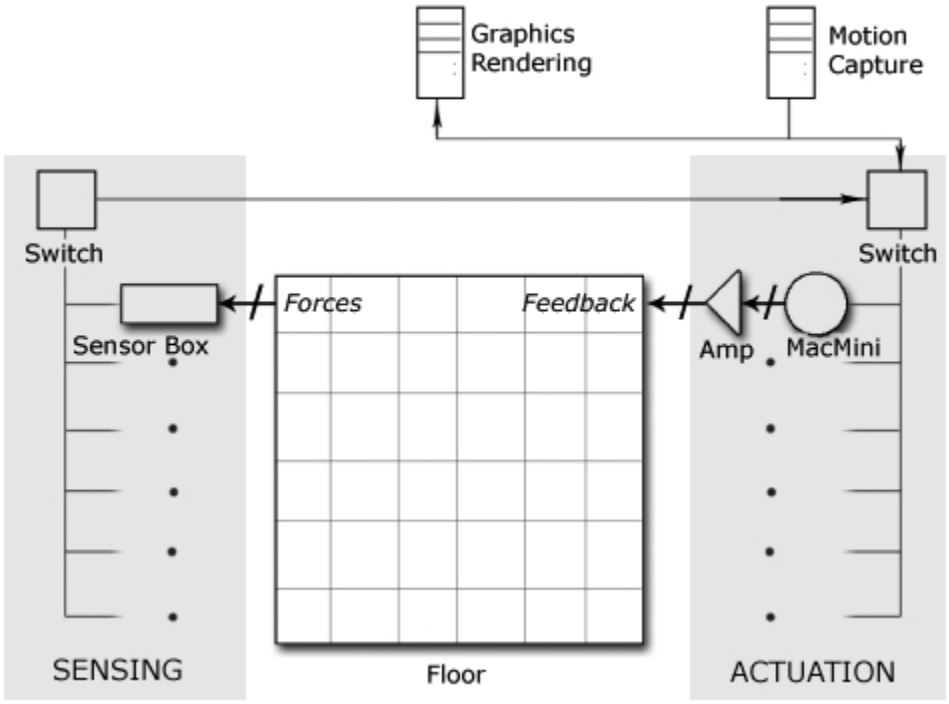

Figure 2.15 A top-down view of the overall placement of components and the logical connections between them.

provides 75 W at 4 Ω per channel. Three such amplifiers power the signals delivered by the six Edirol sound cards allowing for simultaneous and independent feedback of 36 tiles. The components are secured in a server rack as seen in Figure 2.16. Each row of actuators is connected to an amplifier with a custom built twelve-wire snake cable. The rack sits behind the CAVE, unseen from the interaction area.

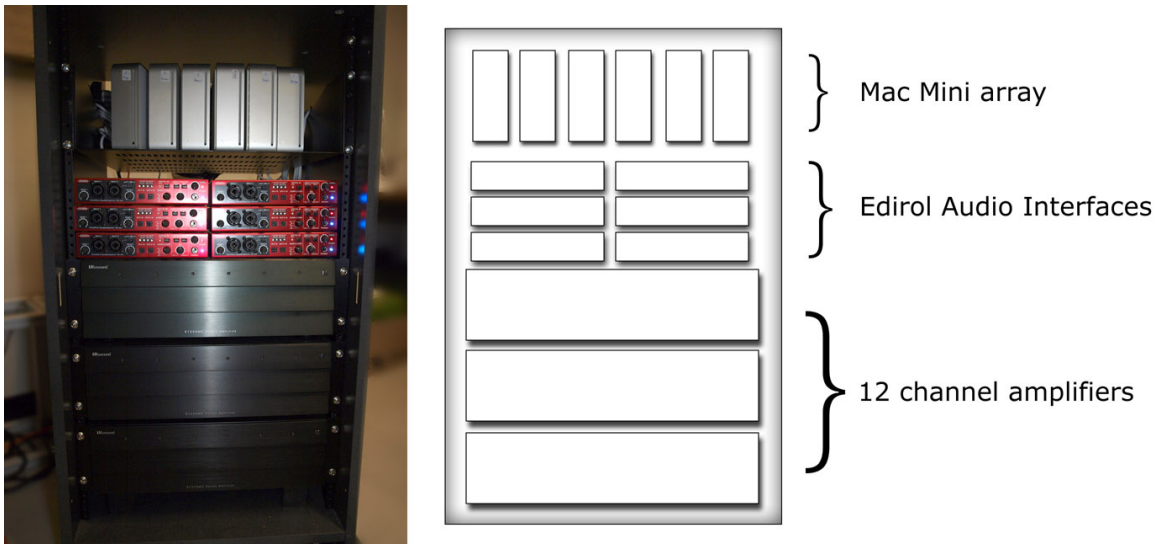

Figure 2.16 The rack of haptic-audio synthesis computers and multi-channel audio hardware.

2.7 Overall Environment

The completed floor is housed within the lab's existing CAVE as shown in Figure 2.18. Our augmented platform adds a fourth display surface that also acts as an interaction device allowing for some interesting applications, which are described in the next chapter. It can supplement existing VR environments by adding realistic multimodal feedback or it can act as the main interface device with graphics from the screens enhancing the overall immersion. The abstraction of its components and the rigidity of construction allow the floor to behave as a regular raised platform when not activated.

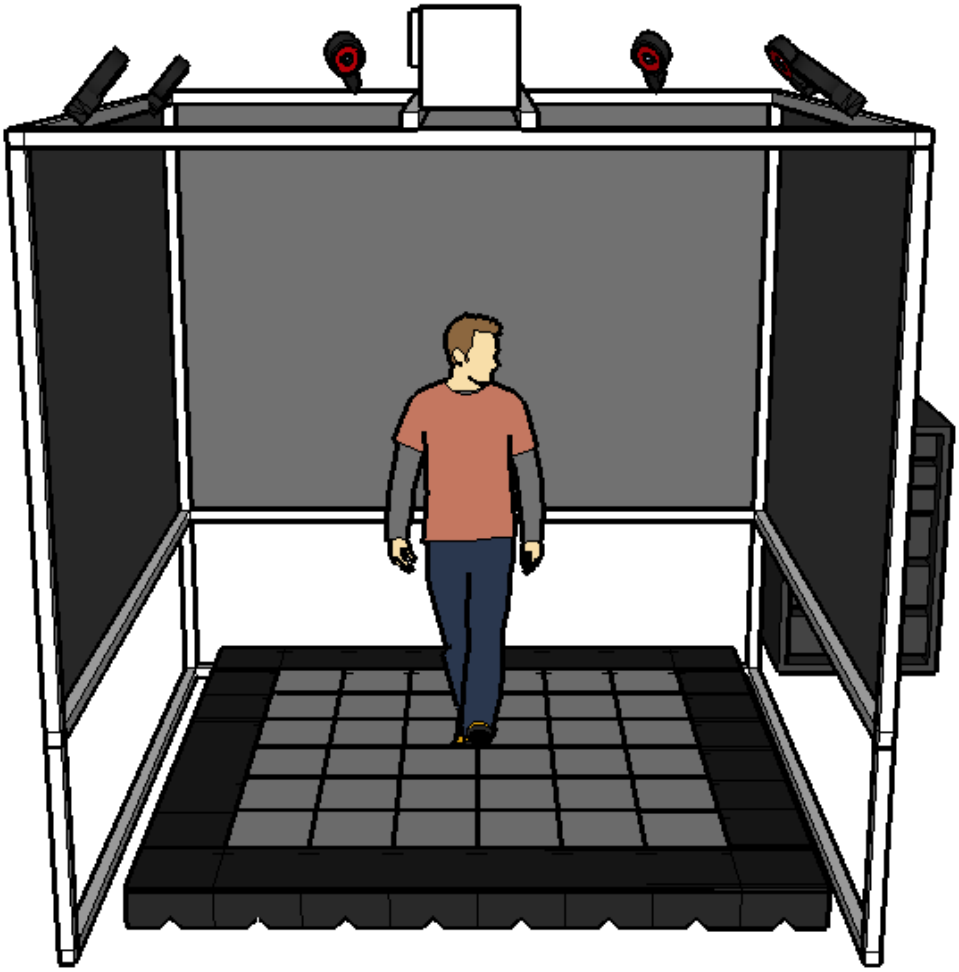

Figure 2.17 Sketch of the completed construction in the lab's existing VE. It includes three back-projected screens and a set of motion capture cameras.

Figure 2.18 The completed floor inside the lab's CAVE.

Chapter 3

Applications [1]

The vibrotactile floor space enables content creation new to the domain of VR. It moves both user input and feedback away from conventional hand-held controllers and computer screens to completely floor-based interaction. Two virtual environments were created using this platform to demonstrate its novel aspects. [2] The development involved adapting the haptic-audio synthesis engine, creating interactive graphics, and managing the communication between those two systems. Also, in contrast to real-world terrains, we describe a preliminary evaluation of abstract vibrotactile icons and how our haptic floor can be used to facilitate testing of such signals under varying conditions.

3.1 Haptic-Audio Synthesis

This section describes the vibration synthesis software used for haptic-audio feedback. Haptic vibrations and audible sounds form two of the three feedback modalities provided

1. Contributions from the author include setup of the system architecture, tuning the synthesis parameters for each material, adapting the deformable snow terrain graphics to interact with the sensing floor, creation of the virtual ice environment, conducting user experiments, and preliminary analysis of test data.
2. Videos can be viewed at http://www.cim.mcgill.ca/sre/projects/niw

by the floor interface used in this project. For many unique terrains, any one of the three modalities would be sufficient for identification. For simulation, however, the system should provide as many modalities as possible to reinforce the illusion.

A simple solution to provide feedback is to play recorded sound files when a sensor reads a value above a set threshold. Although quick to implement, the resulting responses may be perceived as repetitive and unnatural. Our system uses physically based algorithms for the synthesis that offer a more realistic experience than the previously mentioned approach by adapting the feedback to match nuances within each footstep. This method also allows for adjustable semantic parameters that can simulate a wide range of materials. The customizable control of the mapping from stepping forces to feedback stimuli is based on the Sound Design Tools (SDT) library [28] [29].

3.1.1 Sound Design Tools

Crushing granular media provides an ecologically salient form of ground interaction. Granular media includes naturally occurring aggregate materials such as gravel, sand, and snow as well as materials that undergo fracture phenomena such as an aluminum can or a thin sheet of ice. Its range of possible reaction forces span a much richer area compared to a rigid surface such as marble or concrete.

The perceived action of crushing or crumpling a medium can be seen as the superposition of many individual microscopic events. By synthesizing a characteristic vibration for each event, the overall crumpling event is realized. This approach is known as granular synthesis. For this implementation, each grain of sound is described using an impact model [30].

The physical modelling procedure used follows a statistical approximation to physical interactions. A deterministic sequence of events would require much more computing overhead and cause unwanted latency. As shown by Cook [8], statistical approaches offer a

perceptually valid form of feedback that can be generated almost instantaneously.

The system requires an energy input in order to create an output in the form of a vibration. In this case, input energies are the net forces $f(t)$ provided by the user through stepping actions. A control parameter v_f is introduced and represents the change in force over the sampling period and, thus, indicates whether the user is stepping gradually or quickly. It is defined as:

$$v_f = \begin{cases} df/dt, & \text{if } df/dt > 0 \\ 0, & \text{otherwise,} \end{cases} \tag{3.1}$$

where df/dt is the change in force over time. We discard negative values of v_f as they correspond to the upward motion of a step sequence [29].

The statistical approach governing the temporal relations between generated events is a Poisson process:

$$P(\tau) = v_f e^{-v_f \tau} \tag{3.2}$$

The probability that the time interval between events takes the value τ is dependent on v_f, which controls the density of occurrences. For quick steps, v_f is large and produces many events. Likewise, slow changes in sensed forces, such as standing still, result in a low probability of generating events.

3.1.2 Available Parameter Adjustments

The impact and crumpling models were implemented by Bresin, Fontana and Visell as a Max/MSP [3] package and released as the SDT library. Their implementation allows for

3. www.cycling74.com

real-time adjustment of synthesis parameters through a graphical user interface (GUI) of sliders. These values are described in Table 3.1.2.

A starting point for matching material response is to perform a frequency analysis using linear predictive coding (LPC) on a recorded sound sample and setting the frequency modes to approximate the two most dominant spectrum peaks. Other settings are manually tuned to approximate the material's discernible qualities. Figure 3.1 shows the preset values described by the library as "can crushing." The synthesized vibration waveform and spectrogram resulting from a single step are shown in Figure 3.2. Notice that after the initial attack of each sound grain, there are resonant frequencies that decay slowly, thus giving the ringing quality of fracturing metal.

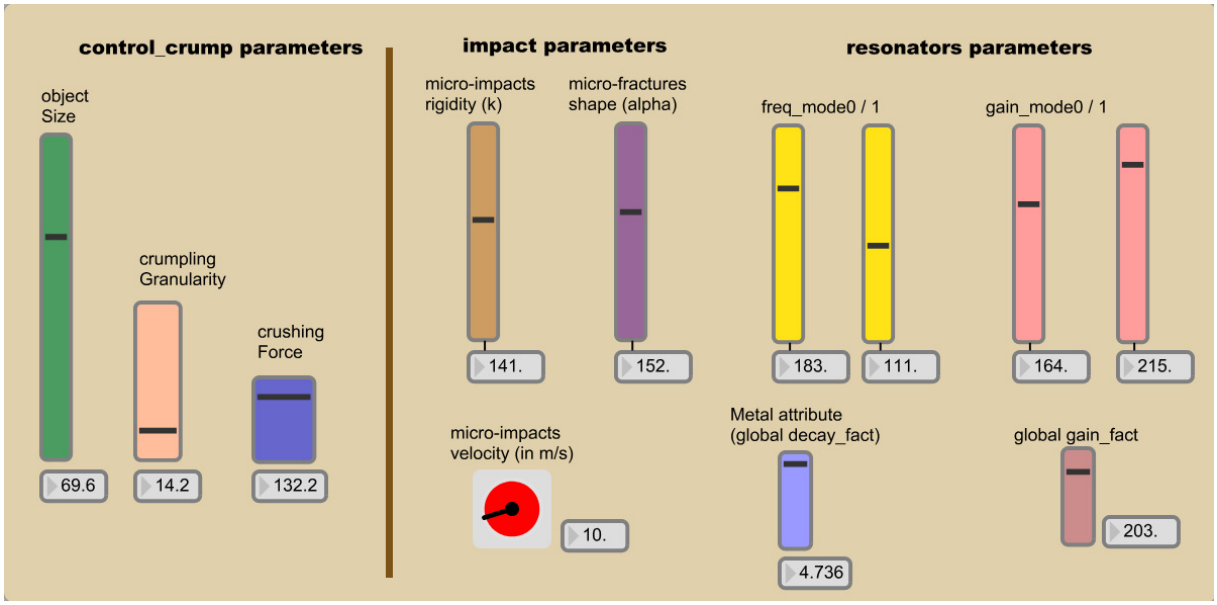

Figure 3.1 Parameter adjustment GUI for the crumpling model. The values shown are for crushing an aluminum can.

Table 3.1 Descriptions of available haptic-audio synthesis parameters.

Name	Range	Description
Impact Parameters		
Micro-impact rigidity	0-255	The resistance of impacting bodies to deformation. Low values denote soft bodies whereas high values denote rigid bodies that resonate longer.
Micro-fractures shape	0-255	Degree of non-linearity in the impact simulation. It can be described as the amount of smoothing, i.e., low values result in harsh sounds.
Micro-impact velocity	0-99	The initial energies of impacting objects. Higher values denote a greater attack amplitude.
Control Crumpling Parameters		
Object size	1-100	Size of object under compression. A small object will be fully crushed with a small number of crumpling events. Large objects can produce many sound events before reaching the limit of being fully compressed.
Crumpling granularity	5-70	How quickly the process evolves. Given the same number of sound grains, the temporal separation between each is controlled by changing this parameter. Small values create fewer events per time period. Bounds were outlined in the SDT library.
Crushing Force	115-150	Scales the amount of force an agent needs to supply in order to cause crumpling events as a percentage. Bounds were outlined in the SDT library.
Resonator Parameters		
Frequency Mode 0/1	0-255	Controls the two center frequencies of the resulting stimuli.
Gain Mode 0/1	0-255	Controls the amplitude of their respective frequencies.
Global Decay	0-8	Regulates signal decay time. Higher values correspond to a metallic ringing signature.
Global Gain	0-255	Amplification of generated signal.

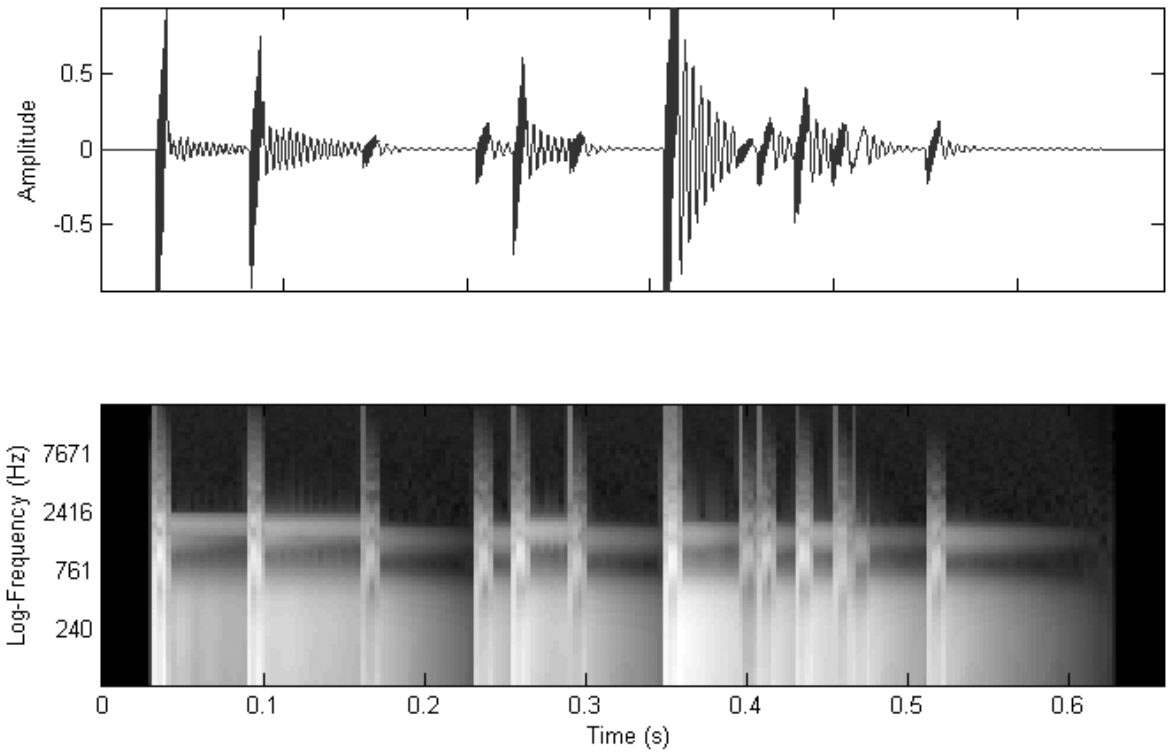

Figure 3.2 Signal analysis of synthesized feedback with can-crushing parameter settings resulting from one step. *Above*: Vibration waveform. *Below*: Associated spectrogram.

3.2 Snow Simulation

A field of freshly fallen snow provides a compelling scenario to illustrate a multitude of sensory cues. Take for example, the senses involved during a step. Before the first foot step, the snow is a bright white colour, evenly covering the ground. As a step is taken and weight applied, the snow begins to compress and a crunching sound is heard. The first few centimeters do not offer much resistance, but as the snow compacts, its structure and trapped air spaces begin to withstand the added pressure. The subject perceives his foot continuing to sink until the compacted layers provide an equal reaction force preventing further compression. An impression from the boot is left in the snow. The next stride feels and sounds slightly different given the variations in the surface and the pressure profile of each footstep. If the foot is dragged along, a smooth channel is left behind.

As described above, the real-life scenario of walking in snow offers a variety of detailed feedback that we aim to recreate within our VE. The following sections describe the implementation.

3.2.1 Haptic-Audio Rendering of Snow

The physics of snow crystal deformation are reviewed by Mellor [31] and more recently by Wu *et al.* [32]. We can draw parallels between the mechanics of real snow deformation and the algorithm that governs the haptic-audio synthesis of virtual snow.

The *crunchy* description of walking in real snow is the result of material failure accompanied by a loss of load-bearing capacity. Resistance to deformation arises from two sources: crystalline strength from formation of ice crystal bonds, and the incompressible air trapped in between them. Wu *et al.* showed that in the event of a uniform plate being dropped onto snow, the combined resistance decelerate the crushing agent unevenly.

This leads to irregularities in the fracturing of ice bonds and discharge of the trapped air that create the characteristic auditory and tactile feedback. This series of discontinuous collapses is referred to as "collapse mechanics" [31].

Further irregularities are introduced from the action of walking, each step producing a unique profile. Collectively, the lumped stochastic crumpling model that generates randomized events following a Poisson process can be taken as an approximation to the real-life series of collapses. The lower frequencies of each synthesized vibration will be perceived by the user's foot as short bursts of force. These are similar to the reaction force felt at the end of each collapse in real snow. Combined with the audible portion of the signal, the synthesized virtual snow illusion is rather convincing. Informal reports suggest that the generated reaction forces distort a user's estimation of material compliance. Some users have admitted to believing that they were sinking into the rigid platform even though no such cues were provided through proprioception.

The most perceptually convincing parameter values for virtual snow are documented in Figure 3.3. They are by no means the only valid values. Minor variations in the settings would produce a slightly different snow. Figure 3.4 shows the synthesized waveform and spectrogram for a single step. Compared to the can-crushing settings, the number of events generated are fewer and the transient vibrations decay faster. The feedback also has fewer high frequency components to match the *muffling* effect that real mounded snow has on propagating sound waves.

3.2.2 Deformable Terrain Rendering

The accompanying graphics projected around the user were based on a height-field implementation of deformable material by Zeng *et al.* [33]. This approach was chosen over a particle system because the latter technique sacrifices interactive update rates for

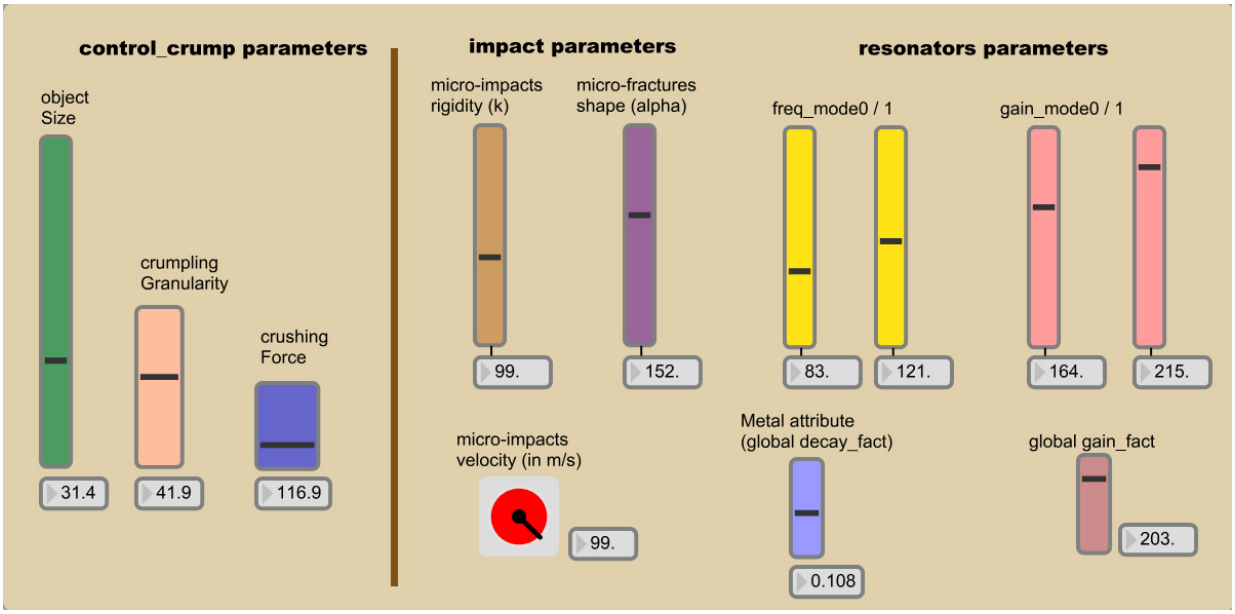

Figure 3.3 Chosen parameter values for the snow simulation.

visual quality. Optimizations that improved upon Zeng's implementation included storing the terrain data in video memory and using the programmable GPU's stream processing architecture to perform dynamic lighting. [4]

Height-field approaches do not compute the collisions between particles of the entire volume of material. The only particles of interest are the ones visible to the user, which exist at the top of the volume. A height-field based surface is defined by a grid of vertices that are displaced vertically according to values stored in a texture, H. Because the vertices and the texture are both stored in video memory, real-time computation of lighting can be performed. Our initial height texture was simply a grey-scale image of clouds. The varying lightness values created a natural wavy snow field as seen in Figure 3.5.

Deformation of the height-field occurs by comparing the volume between a virtual foot

4. Because the pipeline shader programs were written specifically for nVidia graphics cards, the current implementation is limited to work only with GeForce 8000 and above models. Previous generation GeForce cards did not have programmable shaders.

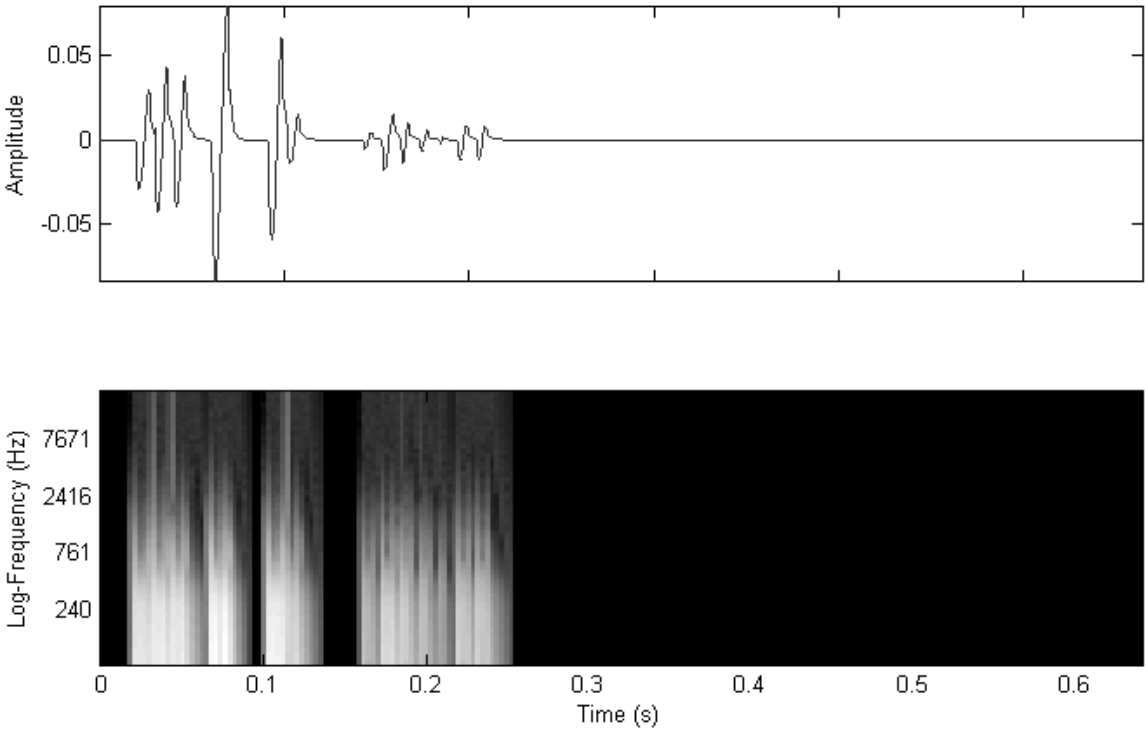

Figure 3.4 Signal analysis of synthesized feedback with snow parameter settings resulting from one step. *Above:* Vibration waveform. *Below:* Associated spectrogram.

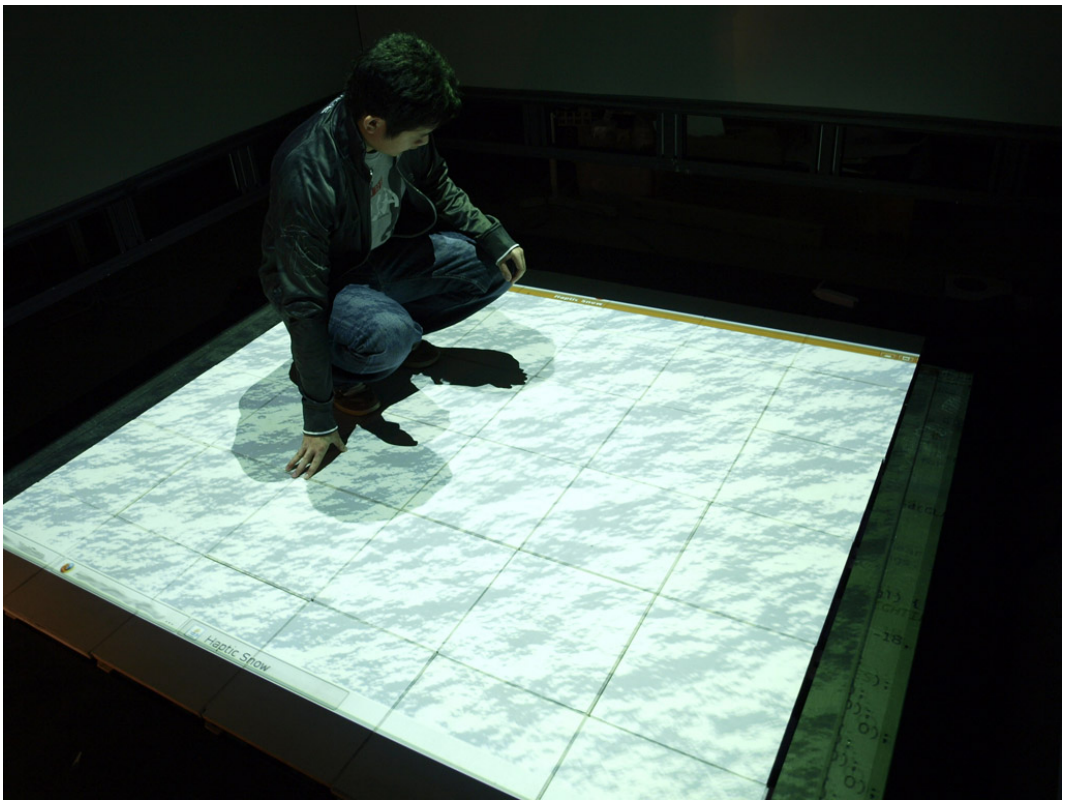

Figure 3.5 The interactive snow field.

and the current height-field texture, H_0. A 3D model of a boot with a hiking tread was created for this purpose. The height of the virtual foot compared to the height-field is determined by the FSR readings. If the force exceeds a predefined threshold, the depth values of the foot are rendered to a texture, F. A subsection of the height-field around the contacting foot, H_{local}, is created to keep the computation time independent of the size of H. F is then compared to H_{local} and a collision map, C, is generated. The difference between C and the original height-field texture, H_0, creates the next frame, H_1, for rendering. The result is the indentation of a foot shaped volume, including details of the tread, in the snow field.

During interaction, the user is unable to see the indentation develop during a step as the visuals occur underneath the shoe. We wanted the graphics to provide mid-step feedback and thus added two Gaussian blurs that were applied to the difference map. A radially symmetric Gaussian blur simulated the mounding of snow at the sides of the footprint and a tangential velocity proportional Gaussian blur simulated the mounding of snow due to horizontal sliding. The mounding effects are seen in Figure 3.6. The rendering procedure is described in full detail by Law *et al.* [34].

Figure 3.6 *Left*: Simple footsteps. *Middle*: A foot drag. *Right*: A foot swipe.

3.2.3 Motion Capture

Exact foot position and orientation were necessary due to the detailed intersection volumes between the foot model and the snow terrain. We would have preferred to keep the interaction free from on-body equipment, but interpolating foot orientation data from the grid of FSRs was insufficiently reliable. An infrared (IR) motion capture system (Vicon or Natural Point Optitrack) supplemented the sensed pressure with the exact position and orientation of each foot. The only equipment worn was an elastic Velcro strap incorporating four IR reflective markers arranged uniquely for each foot. The markers for one foot are seen in Figure 3.7. The user remained uninhibited by cumbersome attachments and was not tethered to any electronics.

Figure 3.7 Vicon markers are attached to the user's feet using an elastic Velcro strap.

Localized deformation for two feet

At each iteration, the values for all 144 FSRs are sent via OSC from the MacMini array to the graphics computer for deformation depth calculations. To relate each FSR value to the correct foot, a set of distance calculations are performed. The task is simple if the

feet are spread far apart, but in many cases, parts of each foot can overlap the same tile. This led to problems when the user moves one foot in the air, such as in mid-stride, and deformations would occur under the moving foot. To reduce this, we introduced a toe and heel position for each foot. FSR values that passed a set threshold are associated with the closest of the four toe and heel positions.

3.2.4 Results

The graphics were rendered on an nVidia Geforce 8800GT card and obtained interactive frame rates of over 75 Hz. The graphical simulation was programmed in Java using the JOGL OpenGL package. [5] Real-time multimodal interaction was achieved allowing users to create a trail of footprints, seen in Figure 3.8, and shoe swipes using both feet. Most participants expressed surprise at the level of realism produced by the simulation. There were some instances of subjects being caught off-guard and in a state of suspended belief, checking to see if their shoe tread matched that of the virtual footprint.

3.3 Ice Simulation

Another scenario that involves numerous characteristic sensory cues is walking on a sheet of ice that is fragile and sensitive to weight changes. The following paragraph describes a possible experience one might have while walking on a real frozen pond.

Imagine approaching a body of water that has frozen over. You are unsure whether the ice is thick enough to support a person's weight, but disregarding all safety concerns, you walk onto the ice in an effort to get to the other side. Your first step is taken cautiously and you find that ice can indeed bear your weight. Looking down, you can see a school of fish

5. jogl.dev.java.net

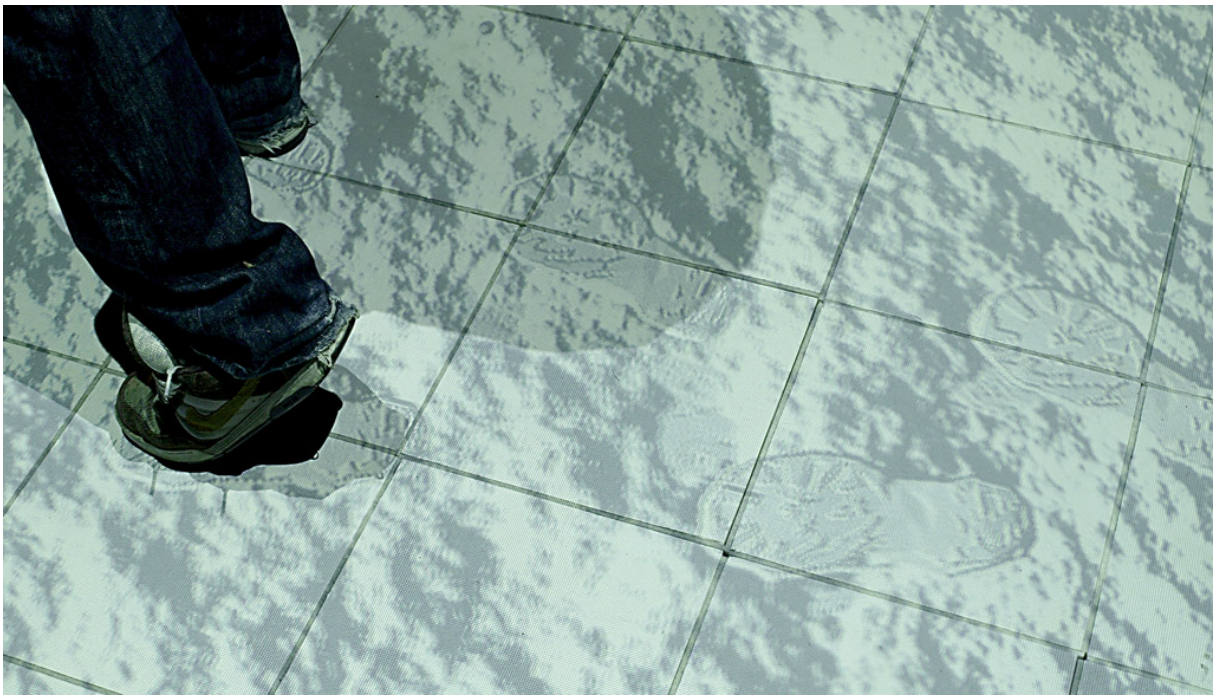

Figure 3.8 A trail of footsteps is left behind by the walker.

swimming underneath the translucent ice. With confidence, you take the next few steps more quickly and all of sudden, you feel a shock against your stepping foot and hear an abrupt snapping sound. You can also see thin white cracks extending from your stepping foot as the ice fractures under the weight of your body. In an attempt to return to the edge, you step back, but cause a second crack. Frightened again and panicking, you leap towards the edge, but fall just short. The landing shatters the immediate area of ice and the surface shakes violently causing the fish to dart away. Fortunately, you make it back to land alive and well.

The virtual ice environment attempts to capture all of the above-mentioned phenomena. This interaction can be quite enjoyable when there is no danger of falling through the ice.

3.3.1 Haptic-Audio Rendering of Ice

An overview of the mechanics of ice fracture under stress is presented by Schulson [35]. Ice fractures propagate in seemingly random directions due to point defects in its crystal structure during the forming process. Under uni-axial pressure, such as a footstep, the stresses incurred cause inelastic crack events. Separation along a series of grain boundaries occurs at the closest point defect. Ice can undergo both ductile and brittle behaviour. At low rates of increasing pressure application, ductile behaviour occurs allowing the ice to increase its load bearing capacity through strain-rate hardening and thermal softening to relax its internal stresses. Ductile behaviour is the reason that an ice sheet, which would normally fail under the weight of a human, can remain intact if the changes in pressure are gradual. However, high speed changes in pressure can cause ice to become brittle and suffer shear failure.

The auditory and tactile feedback can be modelled using the same crumpling stochastic process as the snow simulation. Large-sized cracks are a superposition of many smaller brittle fractures, each with its own grain of vibration. The synthesis parameters chosen for ice fracture are shown in Figure 3.9. The main differences from the can crushing settings are the object size, global decay and resonant frequencies. Fracturing materials have a short snapping sound associated with each failure, thus, the decay parameter was increased to muffle each sound grain almost immediately. The object size parameter was increased to allow for many crack events per step since an ice sheet is not limited to a maximum number of failures unlike can crushing. Lastly, the resonant frequencies were adjusted to match each other to create a thin, hollow sound. The spectrogram of the synthesized feedback in Figure 3.10 shows the short bursts of sound associated with each crumpling event.

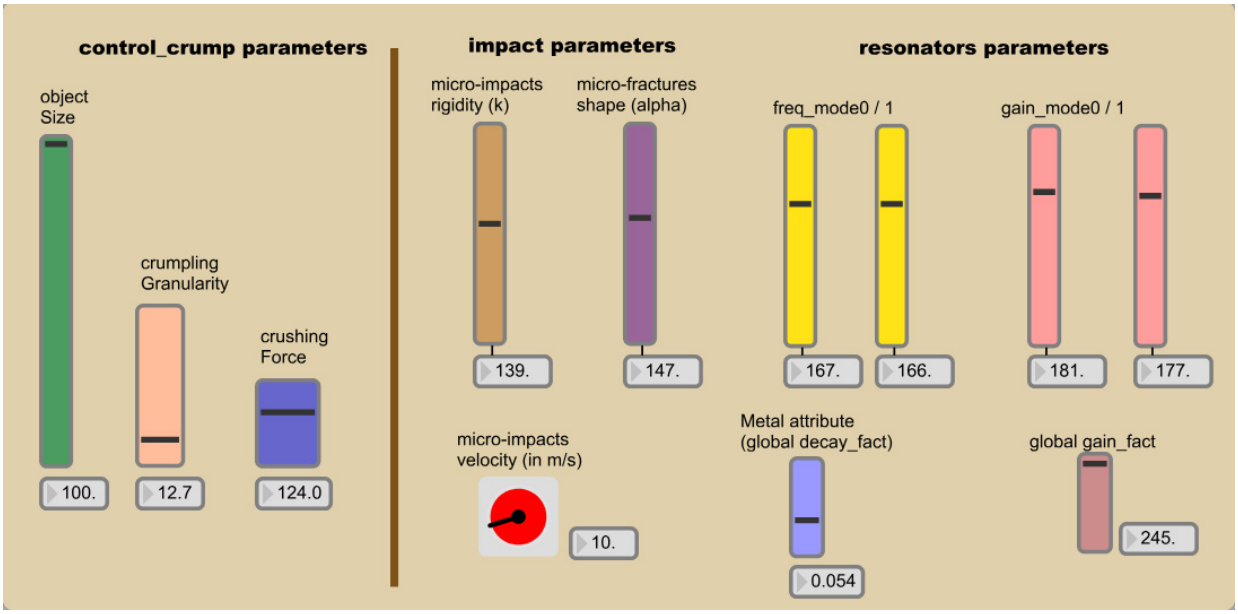

Figure 3.9 Chosen parameter values for the ice simulation.

3.3.2 Visual Crack Rendering

Visual representation of crack propagation due to brittle fracture was developed. The animation must render in real-time and correspond to the audio and haptic feedback. Fracturing of crystalline objects has been studied for computer graphics and has achieved near-photorealistic results [36] [37]. However, the algorithms that exist required considerable computation time and the resulting quality exceeded the amount of realism that seemed necessary for our prototype. Therefore, we developed our own simplified version inspired from those methods.

The cracks should propagate at the same rate as the haptic and audio vibrations being generated to be perceived as simultaneous. Therefore, the animation is triggered every time the program receives a crumpling event – the same event that activates each vibration grain. This approach ensures correlation between all three modalities.

We start by displaying a translucent texture of an ice sheet as shown in Figure 3.11.

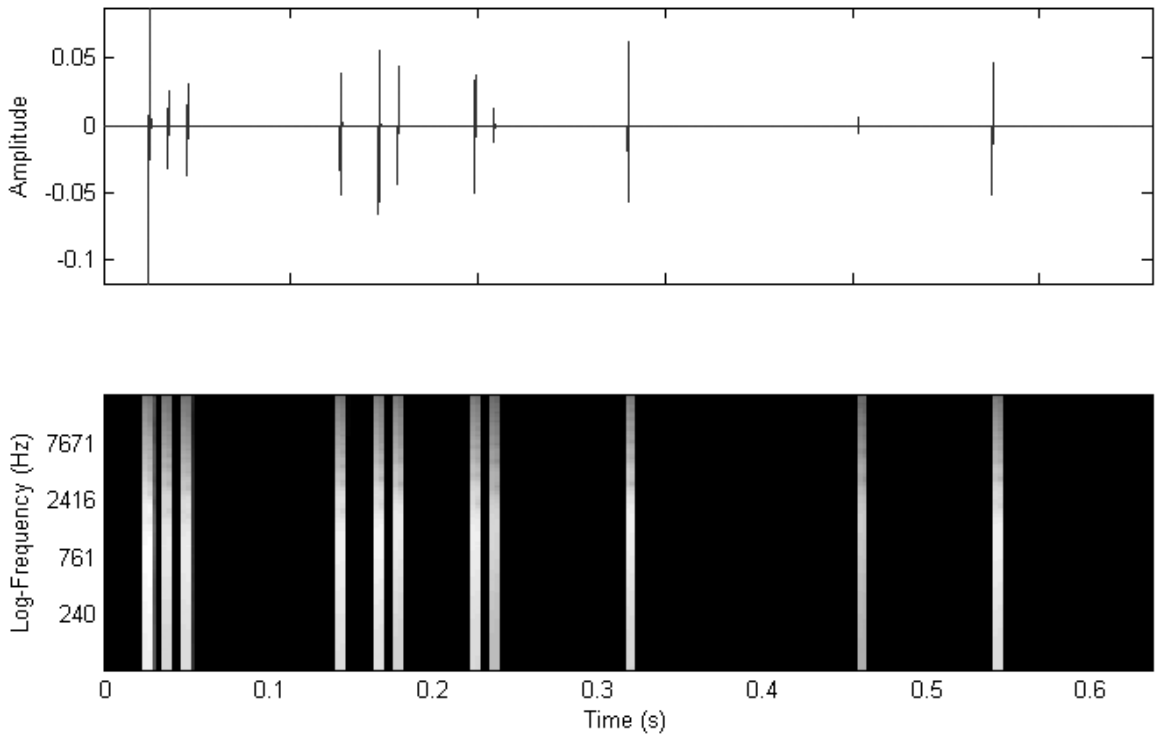

Figure 3.10 Signal analysis of synthesized feedback with ice parameter settings resulting from one step. *Above:* Vibration waveform. *Below:* Associated spectrogram.

Thin white lines represent the crack boundaries and are rendered over top of the ice texture using the following algorithm.

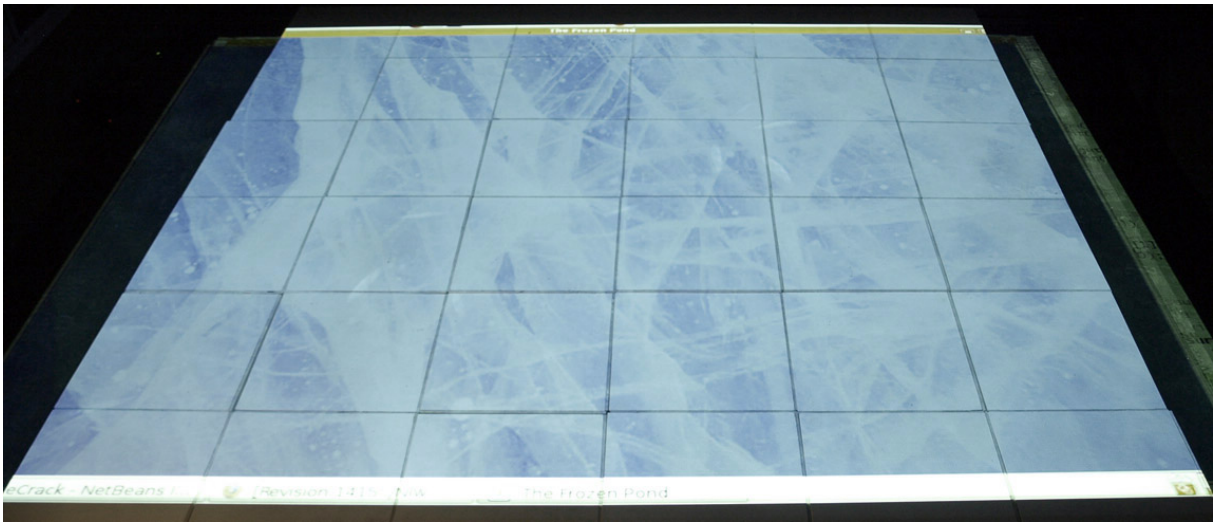

Figure 3.11 The interactive frozen pond surface.

Algorithm

We begin by analyzing the behaviour of a single crack arm or crack front originating from a point c_0. When initiated, the crack arm a has a zero energy value, $E = 0$, associated with it. Each time the arm receives a crumpling event, it increases E by one and creates a new node point c_E such that a mature crack arm is a collection of nodes,

$$a = (c_0, c_1, c_2, \ldots, c_E). \tag{3.3}$$

The arm is visualized by rendering white lines that connect the nodes. The equation governing the position of newly generated nodes is:

$$c_i = c_0 + iD(\hat{n} + \hat{r}) \tag{3.4}$$

where D is the growth distance, or how large to graphically represent each crumpling event. This material constant is defined perceptually. $\hat{n}$ is the arm's propagation direction and $\hat{r}$ is a random direction vector with a Gaussian Normal distribution $N(0, \sigma)$. Adjusting σ controls the amount of jaggedness that occurs. The cracks seen in the figures use $\sigma = 1$ degree.

A crack, C, is initialized at a seed point c_0 with many crack arms such that they share the same origin,

$$C = (a_0, \ldots, a_j), \tag{3.5}$$

where j is uniformly sampled from two to six. Each crack arm's direction vector $\hat{n}_j$ is distributed around a unit circle.

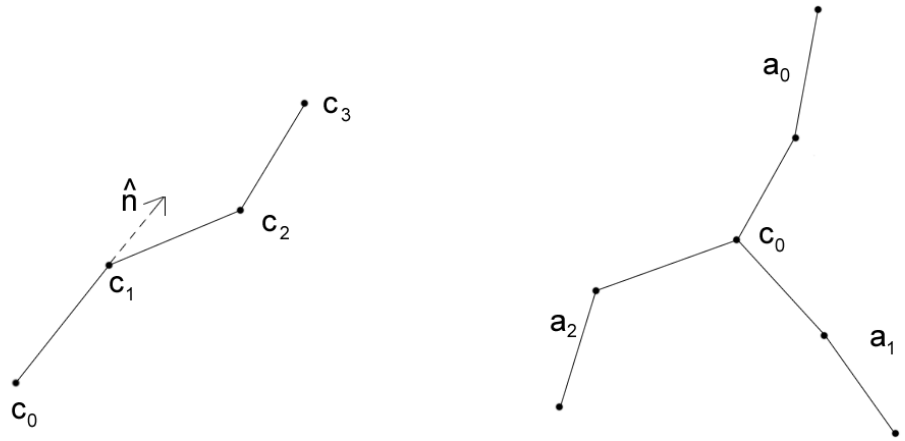

Figure 3.12 *Left*: Nodes of one crack arm and its direction vector. *Right*: Multiple arms of a crack object.

The full rendering of the graphics is the display of all existing cracks over top of the ice texture.

When a crumpling event is received, an FSR identifier value, mapped previously to a location in the projected area, is associated with it. From the knowledge of this location, the program first checks if there are any existing crack seeds within a specified distance $\triangle d$. If there are none, a new crack C_k will be generated. Otherwise, the events will add energy to the nearest C_k, propagating its crack arms a_j^k outwards.

Animation is perceived because all the nodes are preserved. At the instance of a crumpling event, a new furthest point, and thus a new connection line, is generated and the user sees the result as *crack propagation*. Figure 3.13 shows three successive frames to illustrate the applied algorithm.

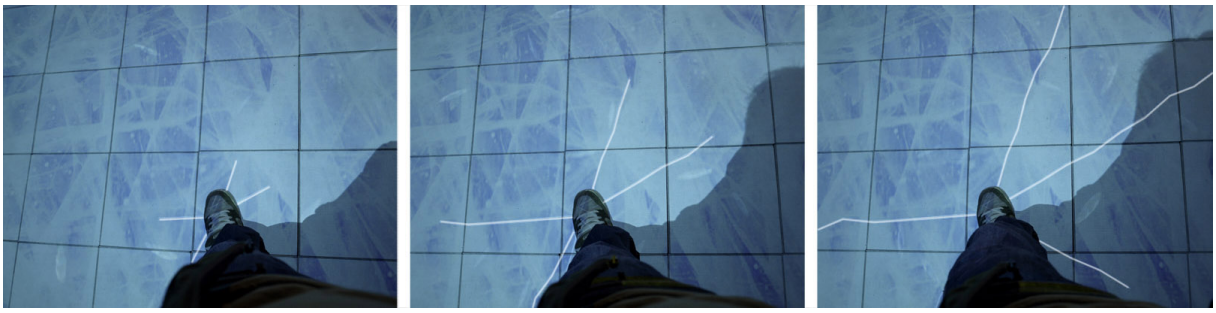

Figure 3.13 The crack arms propagate outwards from the foot. The lines have been enhanced in the photographs to show the effect.

Branching

The phenomena of branching occurs when a crack front encounters a defect. This is modelled by using a branching percentage variable, $B \in (0.0 - 1.0)$. We set $B = 0.1$ to achieve perceptually acceptable results. For any crack C_k, on average, every $1/B$ propagation events it receives creates a new branch arm a_B, as follows.

First, a random arm a_j^k is selected. Its halfway node $c_{E/2}^j$ and direction vector $\hat{n}_j^k$ forms the basis for the branch arm. Branch arm a_B has the initial starting point of $c_{E/2}^j$, a zero energy E_B and a direction vector of $\hat{n}_{jB}^k$ where

$$\hat{n}_{jB}^{k} = \hat{n}_{j}^{k} \pm \pi/4. \tag{3.6}$$

The addition of a 45° angle offset ensures that the new branches propagate in the same general direction as the parent branch, but not directly over top of it. Subsequent branchings can occur from both the original arms or existing branch arms.

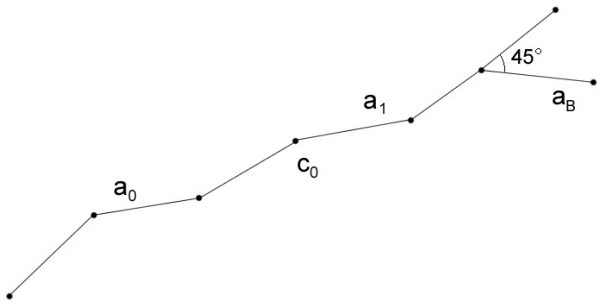

Figure 3.14 Branching occurring on the right crack arm.

3.3.3 Position Sensing

Because footprints are not captured by ice in general, foot orientation is not needed and the interaction could proceed without the aid of a motion capture system. Unlike the snow simulation, which required attaching reflective markers, users could interact with the virtual ice immediately – a feature that could prove important if the simulation were to become an unsupervised installation.

3.3.4 Results

In our initial testing with the snow simulation, we found that users were quickly bored, even though the multimodal experience was highly accurate and conveyed detailed visual, auditory and haptic feedback. We speculated that this was due in large part to the lack of any surprising events. To make the ice simulation more engaging, a few extra features were added. A model of a fish was created and instantiated many times to swim in randomized, straight paths adding a sense of life and movement to the simulation. Some fish can be seen in Figure 3.15, though they are quite difficult to notice in still photographs. They were intentionally made to look faint so as not to distract users from their main activity of cracking ice.

Figure 3.15 The cracking pattern is rendered over top of the ice texture. Circles indicate a few instances of fish.

The ice surface itself holds a surprise for users who extend a crack past a set threshold. First, the tile closest to the crack will be actuated by a sound file that imitates an ice

shatter. The user feels the floor beneath shake violently and hears a sound similar to an explosion. Graphically, as seen in Figure 3.16, a shatter pattern appears at the crack seed point and the fish vacate the area. All fish instances are triggered to triple their speeds and reverse their initial directions. This animation adds to the participants' sense that they are affecting the entire VE. We have seen some startled reactions from participants who were not warned what to expect. After the initial shock, some users wanted to shatter every available crack and enjoyed scaring the fish away.

Figure 3.16 A shatter occurs at one of the crack seed points.

3.4 Haptic Icons Underfoot

Brief tangible stimuli, also known as *haptic icons*, are vibration patterns that have associated meanings. Receiving information through the haptic modality is practical because it is complementary to our senses of sight and sound, which can often be overloaded. On a

busy street, an important message delivered via beeps or a flashing light could become lost within car noises and crowds of pedestrians. The "vibrate" alert feature on cellular phones is a common example of haptic icons, though its vocabulary is quite limited – a short vibration for text messages, repeated long vibrations for a phone call. Visual or hearing impairment adds to the necessity of supplemental feedback modalities. Haptic messages can also be delivered in a discrete manner. Localized on-body vibrations ensure that the information is delivered solely to a single user.

Ground-based haptic feedback can be found in everyday environments. Passive indicators already exist in the form of raised reflective lane markers that cause cars to vibrate violently and textured tiles that demarcate the border of subway platforms. Although passive markers are effective for a singular purpose, "active" haptic markers could modify their feedback to match the current situation and deliver even more information. The type of vibration perceived could, for example, indicate the distance to the next rest stop or the waiting time for an upcoming train.

3.4.1 Motivation

In addition to VEs, the floor interface can serve as a platform for testing systematic information delivery in the form of haptic icons. Unlike ecological surface terrain, these artificial meanings must be specified by the designer and learned by the users. They hold potential in information delivery due to their customization and artificial feel versus terrain. These signals could be embedded in existing ground surfaces and when delivered, the pedestrian would instantly know a vibration is being sent and would interpret it.

A common problem with haptic messages in general is that designers are unsure of how their icons will be perceived under various contexts and end-user scenarios. Users could be under stress or distracted by events around them making it difficult to quickly

recall semantic information. The difference between sitting, standing, and walking could be influential in the interpretation of a message. It would be beneficial for the designers to test their tactile feedback in a controlled virtual simulation.

Our system provides a testing platform well-suited for haptic icons underfoot. The CAVE screens can display images pertaining to a given situation while the floor device mimics a relevent terrain. Haptic icons can be situated anywhere on the floor by specifying those tiles. For example, a simple subway platform scenario could be simulated. Videos of an underground station are projected onto the CAVE screens and a virtual train arrives at predefined intervals. The front two rows of the floor act as the subway tracks and appear black. The back two rows act as the platform and appear grey. The middle rows act as the border and appear yellow. When the border is stepped on, the haptic icons delivered inform the subject to be cautious and that a train is arriving in n minutes. The whole floor rumbles as the train draws close and we can determine the degree that it affects the vibrotactile message. A range of varying conditions can be quickly tested in this manner.

Before attempting such a particular scenario, however, we proposed a simpler experiment that uses the constructed platform to determine whether or not it is indeed possible to recognize a set of ground-based vibrotactile icons. This was motivated in large part to verify that the feet are able to perceive hand-based haptic icon characteristics considering their similar sensory physiologies [38].

3.4.2 Background

The size of the stimuli set recognizable by humans depends on many variables. Location on the body, amount of attention diverted to other tasks, experience and numerous other factors all affect the recognition rate. Studies by MacLean *et al.* [39] and van Erp *et al.* [40] have shown useable sets of 36 and 59 icons respectively through use of musical

metaphors. In these experiments, the vibrations were delivered to the fingers and hands. Recognition rates for arbitrary stimuli delivered to the feet have been less studied, although are predicted to be reduced due to the lower sensitivity of the feet.

3.4.3 Design of Stimulus Set

The multitude of parameters involved in stimulus design is the subject of many studies. Details of the icon design process and icon creation software used for this experiment are described by Visell *et al.* [41]. A total of eight unique stimuli were constructed using a musical paradigm. A single note was created using adjustable parameters and repeated following a distinct rhythmic pattern. The icon design software allowed specification of rhythm, individual note amplitude, repetition of rhythmic pattern, phrase duration, roughness, fundamental frequency, and an overall amplitude envelope. Duration of icons ranged between 1.4 and 2.4 seconds.

3.4.4 Methodology

Setup

Users were asked to wear men's hard-soled shoes provided in various sizes by the experimenters. This was done to reduce the effect of varying footwear between subjects. The platform on which users stood consisted of four tiles that vibrated uniformly. A podium elevated a computer screen and a mouse to a height comfortable for use by a standing person. Closed-form headphones playing pink noise were worn to mask potential auditory cues. The user would initiate stimulus delivery by clicking on selected buttons seen on the experiment program GUI. Although not used in this experiment, the force sensors could be implemented to trigger such signals.

Procedure

The procedure for every participant consisted of six test sessions, each with sixteen identification trials. All eight signals, identified by a number, were presented twice per session in randomized order. Participants were given only five minutes to learn the associations through self-guided selection and feedback. Each identification trial involved a single stimulus presented up to four times depending on the participant. They would select the assumed correct stimulus number and then be shown the answer. This was done to facilitate learning of the associations. An optional one minute break was given to subjects between sessions in case of fatigue during the 20 to 25 minute experiment. Pre-test, post-test questionnaires and the consent form are found in Appendix A.

Subjects

Twelve subjects between the ages of 20 and 39 took part in the experiment. Of those, seven were male and five were female. Nine subjects reported prior musical training. All participants used the same stimulus set, but as noted before, received them in a random order. They were paid $5 each for their participation with a motivational bonus of $50 to the one who achieved the highest recognition rate.

3.4.5 Results

The average identification rate across all testing sessions is summarized in Figure 3.17. The highest identification rate was 68% and the lowest was 28%. The average over all sessions and all participants was 49% with a standard deviation of 12%. Chance performance would correspond to 12.5%. Participant 2 achieved a 94 % recognition rate during the last test session.

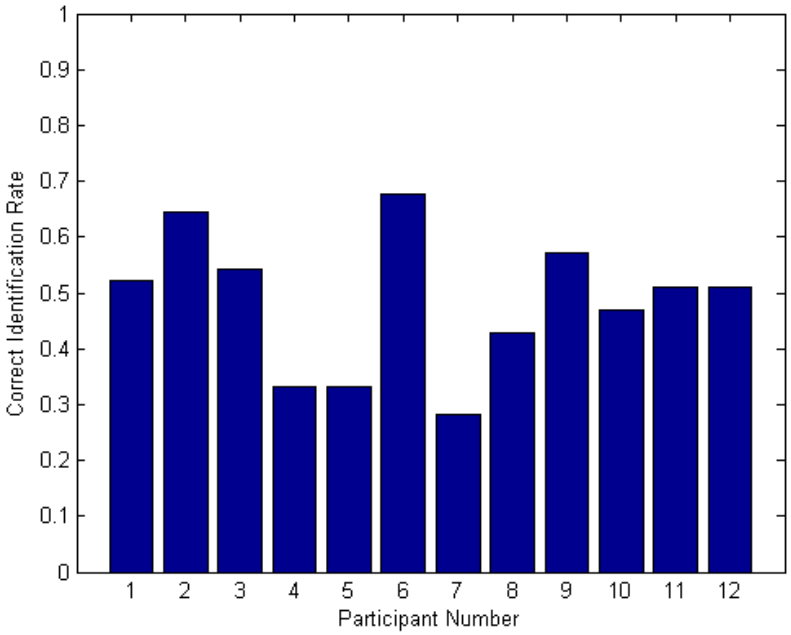

Figure 3.17 Average correct identification rates across all sessions for each subject.

Figure 3.18 presents the overall recognition rate for each stimulus. Stimulus 6 was most easily identified but not by a large margin. Stimulus number 3 and 8 performed the worst, although still higher than chance. From Figure 3.19, we can see the potential for error between pairs of stimuli. Icon number 2 was often confused with number 8. Examining these stimuli, it seems that participants prioritized rhythm as a key identifier. There was also a high number of errors between icons 3 and 4. We suspect that duration was also a major factor. These two stimuli were the longest signals of the set at over two seconds each – other signals were between 1.4 and 2 seconds each.

The rate of learning with standard deviations is shown in Figure 3.20. We see that the peak performance occurred during session four with a recognition rate of 58%. From subject comments, the plateau effect in sessions five and six seemed to be caused by fatigue. Almost all subjects attempted to complete the entire experiment without a break, fearing

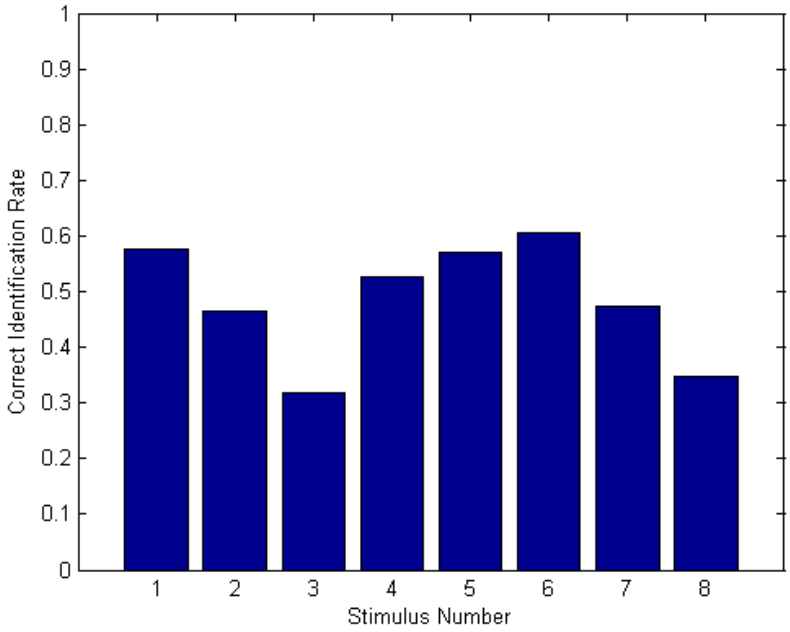

Figure 3.18 Average correct identification rates across all subjects for each stimulus.

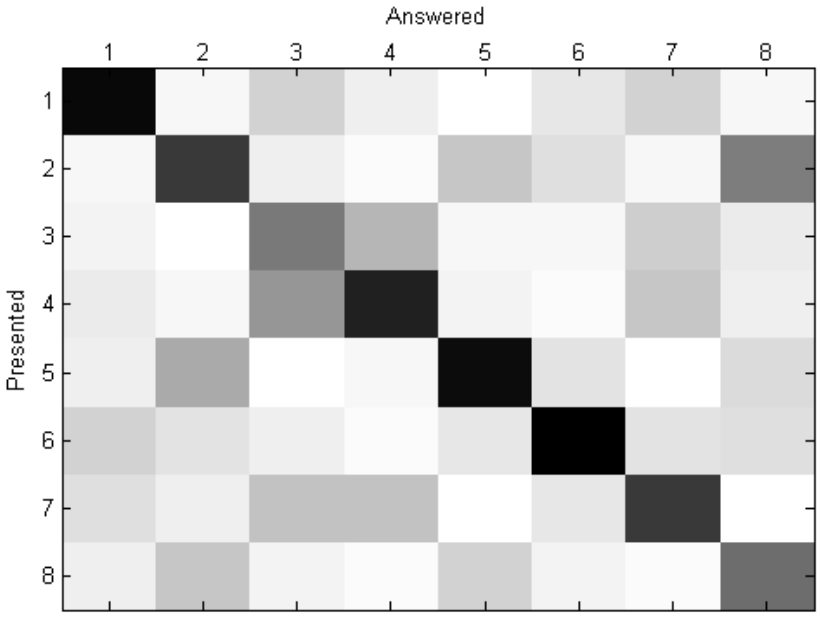

Figure 3.19 Confusion matrix for all subjects indicating number of responses by the darkness of the cell.

loss of learned associations.

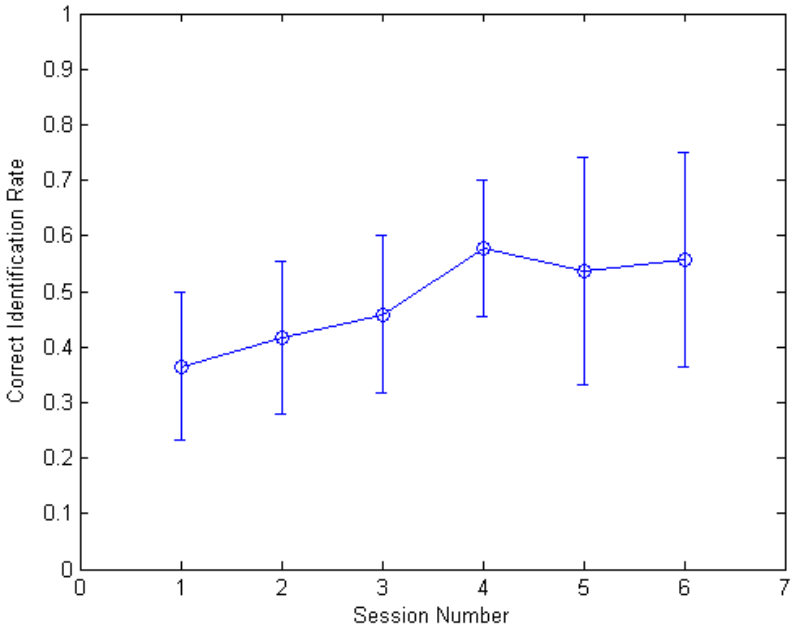

Figure 3.20 Mean recognition rates averaged across all subjects for each session.

This preliminary set of experiments showed that recognizing haptic vibrational icons through the feet was possible given a small stimulus set and a minimal amount of learning. The increasing learning curve indicated that our mental and physical capabilities can adapt to such an interface. All participants were unfamiliar with this type of information transfer but expressed that it did not feel unnatural. On a scale of one (uncomfortable) to five (comfortable), participants rated the interaction at 3.4 with a standard deviation of 1.22.

Chapter 4

Conclusions and Future Work

4.1 Conclusions

An important step in the realization of a multimodal floor interface for virtual environments has been achieved with this project. We began with the aim of improving on available floor-interface designs by adding localized haptic, auditory, and visual feedback presented directly from the ground. Tactile feedback was the key novelty in this project and we wanted to show that it makes a considerable difference in the way a user experiences a VE. We feel that a majority of simulation systems, including ones that use HMDs, can benefit from incorporating a vibrotactile floor. Our design choices in keeping all sensing and actuation embedded into a raised flooring promotes unobtrusive integration into existing systems. When not in use, it blends into the surroundings behaving no differently from common floor tiles.

Each aspect of the hardware for this project went through careful consideration and decisions were made based on a combination of ease of integration, durability, performance and cost. The physical platform, constructed out of affordable housing lumber, provided

a reasonably stable foundation for the sensors and actuators. For future iterations, higher quality lumber should be used as the housing beams exhibited some curvature that complicated the construction phase. Because constant removal of the tiles during the prototyping stage would repeatedly shift the sensors, we temporarily used an average calibration curve for all FSRs. Even so, the sensing proved adequate for providing accurate force readings – at least for our existing applications.

The choice of Clark Synthesis TST vibrotactile actuators, and thus, 30 cm $\times$ 30 cm tiles, created an acceptable vibration resolution while keeping the interactive area a usable size. We noticed, however, that the haptic signal was received differently dependent on the location of the user's foot on the tile. There seemed to be a decline in amplitude as the foot moves towards the edges. This is problematic in that it creates an uneven tactile response over the haptic floor. A stiffer tile material, better actuator coupling, and stronger tile constraints could help minimize this effect. With respect to evaluating the role of haptics compared to graphics and sound, this actuator has difficulty in completely decoupling vibrations that pertain to haptics from vibrations that are audible. Even for low frequency levels below the hearing threshold for most people, 20 Hz, resonances from the tiles and surrounding support can be heard. For experiments that need to isolate single modalities, alternative solutions can be employed. Playing pink noise through headphones can reduce the amount of sound heard and attaching a compliant material, e.g., soft foam, on the underside of shoes can absorb vibrotactile feedback.

Two immersive virtual terrains, snow and ice, were created to provide ecological interactions previously unachievable through conventional systems. These environments were showcased at the largest computer graphics and interactive techniques exhibition, Emerging Technologies of ACM SIGGRAPH 2009 [42]. This event lasted five days with hundreds of people walking on our virtual surfaces and experiencing the potential value of adding an

augmented floor into existing VEs.

Comments from the general public indicated that the level of attainable realism surpassed their expectations. Prior to stepping on the platform, several spectators commented on being intrigued, though puzzled, by the level of amusement expressed by the active participants. There were no buttons to press and no objects to grasp, yet the behaviour of the system was strictly reliant on interaction. We like to stress the simplicity of achieving a successful human-machine feedback loop i.e., perceiving the correct response from an input action, with our simulations. There exist many "haptic" devices that claim to be realistic when they, in fact, require users to concentrate and repeat the action several times in order to interpret what the system is trying to convey. Any extra cognitive load that the user devotes to interpretation detracts from the realism of the system. While using our system, very few participants commented that they had difficulty associating the feedback with the given terrain, although they could be biased from prior descriptions of the VEs. The ice surface emerged as the more popular of the two scenarios; in particular, users were greatly entertained by the shattering event. The ice simulation was also enjoyed by a group of children from a local day-care centre.

Our system also serves as a VR testing platform for ground-based haptic icons. A preliminary perceptual haptic icon experiment was performed to gauge the ability of participants to learn and identify vibration patterns delivered to their feet. Recognition rates were clearly above chance, but our empirical analysis failed to clarify adequately which aspect of the signal needed improvement. However, we were able to show that every participant had the ability to distinguish between the vibrations irrespective of musical training, and observed that they were all comfortable with the interaction. Ground vibrations, provided within context, rather than with arbitrary numerical associations, could prove useful as an alternative channel for information delivery. We have confidence that a scenario merg-

ing both haptic icons and terrain simulation will provide further insight into locomotive interaction.

4.2 Future Work

Many improvements can be made to further enhance the capabilities of our floor platform. More surfaces, such as sand, grass, and gravel, should be implemented in addition to scenarios where the type of terrain and thus, the feedback, vary over time or are modified by the user. A seashore, where the underlying material could change between sand and water due to periodic waves, would demonstrate the adaptability of our VR system. Abstract scenarios such as a floor covered with virtual bubble wrap would be interesting as well. The simulation system, thus far, lacks an integrated development environment and VR features must be programmed from scratch. We have yet to define a standard approach for the graphics software to interface with the haptic-audio synthesis software.

Another improvement would be to discard motion tracking in favour of purely ground-based sensing. We encountered many situations in which the motion capture cameras would lose sight of the markers for a few frames because it was occluded by the user's legs during locomotion. With additional participants, the frequency of dropped tracking is likely to increase. The need for detailed footprints in environments such as snow and mud would require algorithms to predict the exact position and orientation of the feet from force data. Preliminary work from the lab indicates that there are several constraints from the human body and the FSR configuration that can be exploited for accurate prediction.

Shadows remain a slight distraction in our VR setting. Since the projectors overlap, it is possible to generate two separate video signals. One could modify the graphics so that the projectors compensate for shadows by reducing the brightness in overlapping areas.

One approach to predicting the shape and location of shadows uses cameras to capture the position and size of the occlusion. In our setup, the approximate position of the user is already tracked with the embedded force sensors. Using a generic set of dimensions for a human body, shadows can be predicted and compensated. Audet and Cooperstock [43] have already shown success in this regard with a moving occluding object in front of a video projection.

The floor interface can be extended to domains beyond environment simulation to take advantage of its ability to display tactile icons. Floor-based interaction techniques such as StepWIM [44] and WisdomWell [17] can benefit from additional auditory and haptic feedback. Beyond games, the device can be used in the study of virtualized floor controls. Many operations in dentistry, surgery, and automotive guidance require blind foot control because both the hands and the eyes are occupied. In these cases, active haptic and auditory feedback could be prototyped through virtualization to improve functionality, operation speed, and reliability.

Appendix A

User Testing Documents

CONSENT FORM

You are being invited to participate in an experiment run by Yon Visell and Alvin Law, and supervised by Dr. Jeremy Cooperstock of the Centre for Intelligent Machines. The study evaluates the identifiability, of different sensations you will feel as you step onto a vibrating, but otherwise stationary, tile. You will be asked to wear headphones playing noise to mask any sound cues and wear dress shoes that we provide.

The safety concerns of this study are minimal. The device will not feel much stronger than the sensation of stepping onto everyday ground surfaces in your shoes. The researcher that designed this study has used this device extensively and has encountered nothing of concern. Every effort has been made to prepare safe and comfortable experimental conditions for you.

The experiment will last between 30 minutes and an hour, depending on the pace you set. You will have adequate breaks to rest while the bumping device is adjusted twice. You will be paid for your participation. For analysis purposes, we will ask you for information including your age, sex, level of musical training, and dominant foot. This information and your identity will remain completely confidential in any report(s) pertaining to the results of this study. Please note that you are free to withdraw from this study at any time, and that you are entitled to have the researcher explain to you the purpose of the study after you have completed it.

Finally, should you have any comments or concerns about this study, you may contact Yon Visell at 555-555-5555 (email@email.com), Alvin Law at 555-555-5555 (email@email.com) or Professor Cooperstock at (email@email.com).

I have read and understood this consent form. I have agreed to participate voluntarily in this study.

Participant's name and signature: _____

Today's date: _____

Pre-Test Questionnaire

Participant #: _____

Occupation: _____

Age: _____

Gender: M / F

Dominant Foot: L / R

Shoe-size: _____

Do you have any musical experience?
Please describe (which instrument, including dancing, and for how many years):

_____

_____

_____

How sensitive would you rate your feet?

☐ Very sensitive
☐
☐ Average
☐
☐ Insensitive (e.g. from calluses due to barefoot activities)

How much time would you expect you would require to learn a set of 8 arbitrary pair-associations (e.g. number to letter)?

☐ Under a minute
☐ A few minutes
☐ Ten minutes
☐ Longer

Thank You!

Post-Test Questionnaire

Subject #: _____

How hard did you find the first run?

Very easy 1 2 3 4 5 Very Hard

How hard did you find the last run?

Very easy 1 2 3 4 5 Very Hard

How did you find the vibrations?

Uncomfortable 1 2 3 4 5 Comfortable

How unusual did the vibrations feel?

Very Unusual 1 2 3 4 5 Not Unusual At All

Did you close your eyes when feeling the vibrations? □ Yes □ No

Was there a strategy you used to remember the vibrations?

_____

_____

Were there any vibrations that you thought were especially easy or hard to distinguish?

_____

_____

Do you have any final comments or suggestions for improvement?

_____

_____

We appreciate your participation!

Bibliography

[1] M. Slater and A. Steed, "A virtual presence counter," *Presence: Teleoperators & Virtual Environments*, vol. 9, no. 5, pp. 413–434, 2000.

[2] C. Cruz-Neira, D. Sandin, and T. DeFanti, "Surround-screen projection-based virtual reality: the design and implementation of the CAVE," in *Proceedings of the 20th annual conference on Computer graphics and interactive techniques*, p. 142, ACM, 1993.

[3] B. Buxton and G. Fitzmaurice, "HMDs, caves & chameleon: a human-centric analysis of interaction in virtual space," *ACM SIGGRAPH Computer Graphics*, vol. 32, no. 4, pp. 69–74, 1998.

[4] M. Wozniewski, Z. Settel, J. Cooperstock, S. Technologiques, and Q. Montréal, "A paradigm for physical interaction with sound in 3-D audio space," in *Proceedings of International Computer Music Conference (ICMC)*, 2006.

[5] E. Miranda, R. Kirk, and M. Wanderley, *New digital musical instruments: control and interaction beyond the keyboard*. AR Editions, Inc., 2006.

[6] R. Pinkston and K. McQuilken, "A Touch-Sensitive MIDI Dance Floor," in *Proceedings of the International Computer Music Conference (ICMC'95)*, pp. 224–225, 1995.

[7] J. Paradiso, C. Abler, K.-y. Hsiao, and M. Reynolds, "The magic carpet: physical sensing for immersive environments," in *CHI '97: CHI '97 extended abstracts on Human factors in computing systems*, (New York, NY, USA), pp. 277–278, ACM, 1997.

[8] P. Cook, "Modeling bills gait: Analysis and parametric synthesis of walking sounds," in *Proceedings of the AES 22nd International Conference on Virtual, Synthetic, and Entertainment Audio*, pp. 73–78, Citeseer, 2002.

[9] N. Griffith and M. Fernstrom, "LiteFoot: A floor space for recording dance and controlling media," in *Proceedings of the 1998 International Computer Music Conference*, pp. 475–481, 1998.

[10] R. J. Orr and G. D. Abowd, "The smart floor: a mechanism for natural user identification and tracking," in *CHI '00: CHI '00 extended abstracts on Human factors in computing systems*, (New York, NY, USA), pp. 275–276, ACM, 2000.

[11] R. Headon and R. Curwen, "Movement awareness for ubiquitous game control," *Personal Ubiquitous Comput.*, vol. 6, no. 5-6, pp. 407–415, 2002.

[12] B. Richardson, K. Leydon, M. Fernstrom, and J. A. Paradiso, "Z-tiles: building blocks for modular, pressure-sensing floorspaces," in *CHI '04: CHI '04 extended abstracts on Human factors in computing systems*, (New York, NY, USA), pp. 1529–1532, ACM, 2004.

[13] P. Srinivasan, D. Birchfield, G. Qian, and A. Kidané, "A pressure sensing floor for interactive media applications," in *Proceedings of the 2005 ACM SIGCHI International Conference on Advances in computer entertainment technology*, pp. 278–281, Citeseer, 2005.

[14] S. Jorda, M. Kaltenbrunner, G. Geiger, and R. Bencina, "The reactable*," in *Proceedings of the International Computer Music Conference (ICMC 2005), Barcelona, Spain*, pp. 579–582, Citeseer, 2005.

[15] T. Delbrück, A. M. Whatley, R. Douglas, K. Eng, K. Hepp, and P. F. M. J. Verschure, "A tactile luminous floor for an interactive autonomous space," *Robot. Auton. Syst.*, vol. 55, no. 6, pp. 433–443, 2007.

[16] P. Krogh, M. Ludvigsen, and A. Lykke-Olesen, "Help Me Pull That Cursor-A Collaborative Interactive Floor Enhancing Community Interaction," *AJIS*, vol. 75, 2004.

[17] K. Grønbæk, O. Iversen, K. Kortbek, K. Nielsen, and L. Aagaard, "IGameFloor: a platform for co-located collaborative games," in *Proceedings of the international conference on Advances in computer entertainment technology*, pp. 64–71, ACM New York, NY, USA, 2007.

[18] I. Choi and C. Ricci, "Foot-mounted gesture detection and its application in virtual environments," in *Systems, Man, and Cybernetics, 1997. 'Computational Cybernetics and Simulation'., 1997 IEEE International Conference on*, vol. 5, pp. 4248–4253 vol.5, Oct 1997.

[19] J. Paradiso, E. Hu, and K.-y. Hsiao, "Instrumented footwear for interactive dance," in *Proc. of the XII Colloquium on Musical Informatics*, pp. 89–92, Sept 1998.

[20] X. Fu and D. Li, "Haptic shoes: representing information by vibration," in *ACM International Conference Proceeding Series; Vol. 109*, pp. 47–50, Australian Computer Society, Inc. Darlinghurst, Australia, Australia, 2005.

[21] M. Frey, "CabBoots: shoes with integrated guidance system," in *Proceedings of the 1st international conference on Tangible and embedded interaction*, p. 246, ACM, 2007.

[22] M. Magana and R. Velazquez, "On-shoe tactile display," in *IEEE International Workshop on Haptic Audio visual Environments and Games, 2008. HAVE 2008*, pp. 114–119, 2008.

[23] Y. Visell, J. Cooperstock, and K. Franinovic, "The EcoTile: An Architectural Platform for Audio-Haptic Simulation in Walking," in *Proc. of the 4th Intl. Conf. on Enactive Interfaces (ENACTIVE07), Grenoble, France*, 2007.

[24] J. Castet and J. Florens, "A Virtual Reality Simulator Based on Haptic Hard Constraints," *Lecture Notes in Computer Science*, vol. 5024, p. 918, 2008.

[25] B. Giordano, S. Mcadams, Y. Visell, J. Cooperstock, H. Yao, and V. Hayward, "Non-visual identification of walking grounds," *Journal of the Acoustical Society of America*, vol. 123, no. 5, p. 3412, 2008.

[26] K. Kuchenbecker, J. Fiene, and G. Niemeyer, "Improving contact realism through event-based haptic feedback," *IEEE Transactions on Visualization and Computer Graphics*, vol. 12, no. 2, pp. 219–230, 2006.

[27] J. Russ, *The image processing handbook*. CRC press, 2006.

[28] F. Fontana and R. Bresin, "Physics-based sound synthesis and control: crushing, walking and running by crumpling sounds," in *Proc. Colloquium on Musical Informatics,(Florence, Italy)*, pp. 109–114, 2003.

[29] R. Bresin, S. Delle Monache, F. Fontana, S. Papetti, P. Polotti, and Y. Visell, "Auditory feedback through continuous control of crumpling sound synthesis," in *Proc. Human Factors in Computing Systems Conference, Florence, Italy*, 2008.

[30] F. Avanzini and D. Rocchesso, "Controlling material properties in physical models of sounding objects," in *Proc. Int. Computer Music Conf.(ICMC01)*, Citeseer, 2001.

[31] M. Mellor, "A review of basic snow mechanics," in *Proc. Int. Symp. Snow Mechanics, Grindelwald, IAHS Publ*, vol. 114, pp. 251–291, 1975.

[32] Q. Wu, Y. Andreopoulos, S. Xanthos, and S. Weinbaum, "Dynamic compression of highly compressible porous media with application to snow compaction," *Journal of Fluid Mechanics*, vol. 542, pp. 281–304, 2005.

[33] Y. Zeng, C. Tan, W. Tai, M. Yang, C. Chiang, and C. Chang, "A momentum-based deformation system for granular material," *Computer Animation and Virtual Worlds*, vol. 18, 2007.

[34] A. Law, B. Peck, Y. Visell, P. Kry, and J. Cooperstock, "A multi-modal floor-space for experiencing material deformation underfoot in virtual reality," in *Haptic Audio visual Environments and Games, 2008. HAVE 2008. IEEE International Workshop on*, pp. 126–131, Oct. 2008.

[35] E. Schulson, "The structure and mechanical behavior of ice," *JOM Journal of the Minerals, Metals and Materials Society*, vol. 51, no. 2, pp. 21–27, 1999.

[36] H. N. Iben and J. F. O'Brien, "Generating surface crack patterns," in *SCA '06: Proceedings of the 2006 ACM SIGGRAPH/Eurographics symposium on Computer animation*, (Aire-la-Ville, Switzerland, Switzerland), pp. 177–185, Eurographics Association, 2006.

[37] M. Pauly, R. Keiser, B. Adams, P. Dutré, M. Gross, and L. J. Guibas, "Meshless animation of fracturing solids," in *SIGGRAPH '05: ACM SIGGRAPH 2005 Papers*, (New York, NY, USA), pp. 957–964, ACM, 2005.

[38] M. Trulsson, "Mechanoreceptive afferents in the human sural nerve," *Experimental Brain Research*, vol. 137, no. 1, pp. 111–116, 2001.

[39] K. MacLean and M. Enriquez, "Perceptual design of haptic icons," in *Proceedings of Eurohaptics*, pp. 351–363, Citeseer, 2003.

[40] J. van Erp and M. Spapé, "Distilling the underlying dimensions of tactile melodies," in *Proceedings of Eurohaptics*, vol. 2003, pp. 111–120, 2003.

[41] Y. Visell, A. Law, and J. R. Cooperstock, "Toward iconic vibrotactile information display using floor surfaces," in *WHC '09: Proceedings of the World Haptics 2009 - Third Joint EuroHaptics conference and Symposium on Haptic Interfaces for Virtual Environment and Teleoperator Systems*, (Washington, DC, USA), pp. 267–272, IEEE Computer Society, 2009.

[42] A. W. Law, J. W. Ip, B. V. Peck, Y. Visell, P. G. Kry, and J. R. Cooperstock, "Multimodal floor for immersive environments," in *SIGGRAPH '09: ACM SIGGRAPH 2009 Emerging Technologies*, (New York, NY, USA), pp. 1–1, ACM, 2009.

[43] S. Audet and J. Cooperstock, "Shadow removal in front projection environments using object tracking," in *Proceedings of the IEEE Workshop on Projector Camera Systems (PROCAMS 2007)*, Citeseer, 2007.

[44] J. LaViola Jr, D. Feliz, D. Keefe, and R. Zeleznik, "Hands-free multi-scale navigation in virtual environments," in *Proceedings of the 2001 symposium on Interactive 3D graphics*, pp. 9–15, Citeseer, 2001.